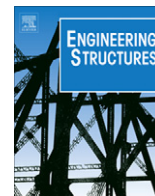


Contents lists available at [SciVerse ScienceDirect](http://SciVerse.ScienceDirect.com)

Engineering Structures

journal homepage: www.elsevier.com/locate/engstruct

Finite element model updating of a bowstring-arch railway bridge based on experimental modal parameters

D. Ribeiro^{a,*}, R. Calçada^b, R. Delgado^b, M. Brehm^c, V. Zabel^d^a School of Engineering, Polytechnic of Porto, Rua Dr. Bernardino de Almeida 431, 4200-072 Porto, Portugal^b Faculty of Engineering, University of Porto, Rua Dr. Roberto Frias, 4200-465 Porto, Portugal^c Université Libre de Bruxelles, Avenue Franklin Roosevelt 50, 1000 Brussels, Belgium^d Institute of Structural Mechanics, Bauhaus-University Weimar, Marienstraße 15, 99423 Weimar, Germany

ARTICLE INFO

Article history:

Received 23 September 2011

Revised 31 January 2012

Accepted 1 March 2012

Keywords:

Finite element model updating
 Railway bridge
 Bowstring-arch
 Experimental modal parameters
 Genetic algorithm
 Experimental validation

ABSTRACT

This article describes the calibration of the numerical model of a bowstring-arch railway bridge based on modal parameters. An ambient vibration test allowed the identification of the natural frequencies, mode shapes and damping coefficients of several global and local modes of vibration of the bridge by the application of an output-only technique based on the enhanced frequency domain decomposition method. The calibration was performed using a genetic algorithm that allowed obtaining the optimal values of fifteen parameters of the numerical model. For the mode pairing, a new technique based on the calculation of the modal strain energy was used. The stability of a significant number of parameters, considering different initial populations, proved the robustness of the adopted algorithm in the scope of the optimization of the numerical model. The updated numerical model was validated based on an experimental test for the characterization of the modulus of deformability of the concrete and a dynamic test under railway traffic. The results showed an excellent agreement between numerical and experimental results.

© 2012 Elsevier Ltd. All rights reserved.

1. Introduction

Railway bridges are structures subjected to high intensity moving loads, where the dynamic effects can reach significant values. At present, these effects are being given greater importance due to the increase of the circulation speed, not only in conventional lines but also in new lines, such as the case of high speed railway lines.

In structures with complex behavior the evaluation of these effects is performed by means of dynamic analyses using finite element (FE) models. The process of developing a FE model of a structure involves assumptions and simplifications that may cause errors. These errors are usually related to the inaccuracy in the FE model discretisation, uncertainties in geometry and boundary conditions and variation in the material properties.

Therefore, the accuracy of the FE model strongly depends on the experimental validation of the numerical results that is usually performed by means of static or quasi-static measurements based on load tests [1,2], dynamic measurements based on ambient vibration or forced vibration tests [3,4], or a combination of static and dynamic measurements [5]. In recent years, in situ dynamic

testing has been used and reported by several authors [3,6–9] in the scope of the identification of the modal parameters of structures, namely the natural frequencies and mode shapes. Experimental modal data is also perturbed by measurement errors typically related with the environmental variability (such as temperature and wind), the variability in operational conditions during the measurements (e.g. traffic) and errors with measured signals and post-processing techniques [10,11]. Despite the presence of the referred errors it is generally assumed that the experimental data is a better representation of the structural behavior than the initial estimations from the FE model [12].

Finite element model updating, also known as calibration of a finite element model, is a procedure to determine uncertain parameters in the initial model based on experimental results to achieve a more suitable updated model of the structure [13]. Updated models can be used for the prediction of dynamic responses under new load scenarios, for damage identification, to design health monitoring systems, as well as for improved remaining lifetime predictions [8,14]. There are basically two distinct finite element model updating methodologies in structural dynamics: the direct [15] and the iterative methods [16–18]. The direct methods directly update the elements of the stiffness and mass matrices in a one-step procedure. In this method the experimental modal properties can be exactly represented by the updated system matrices. Unfortunately, the updated system matrices have little physical meaning, and cannot be related to physical properties of the finite

* Corresponding author. Tel.: +351 22 508 1901; fax: +351 22 508 1446.

E-mail addresses: drr@isep.ipp.pt (D. Ribeiro), ruiabc@fe.up.pt (R. Calçada), rdelgado@fe.up.pt (R. Delgado), maik.brehm@ulb.ac.be (M. Brehm), volkmar.zabel@uni-weimar.de (V. Zabel).

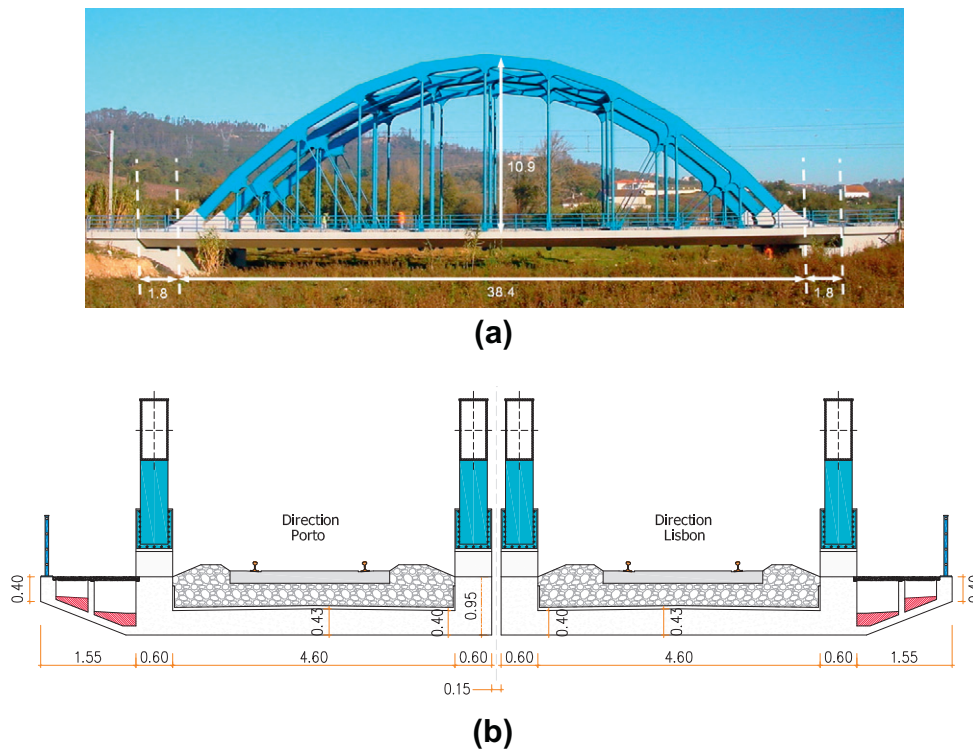


Fig. 1. São Lourenço bridge: (a) lateral view e (b) cross-section of the deck.

element model [13]. The iterative methods are typically related to a penalty function, which is improved by a step-by-step approach. This approach is more flexible in its application as the physical properties of the finite element model can be updated.

Ref. [14] distinguished the solving algorithms for model updating in sensitivity-based methods and optimization-based methods. In the context of optimization-based model updating, the penalty function denotes the objective function based on the discrepancy between numerically obtained and experimentally derived features, such as natural frequencies or modal deflections. The uncertain parameters that need to be updated are material properties or geometrical dimensions, for example. Applications of such methods in the scope of model updating of railway bridges were referred by Chellini and Salvatore [19], Liu et al. [20] and Cantieni et al. [17,21].

Concerning the optimization algorithm, several methods are available to solve the optimization problem. These include gradient-based methods (quasi-Newton, sequential quadratic programming, augmented Lagrangian, etc.) [22], response surface methods [23] and nature inspired algorithms (e.g., genetic algorithm, evolutionary strategies, particle swarm optimization) [10,24]. The genetic algorithm, used in the present work, is not a regularly reported and referenced methodology in the scope of model updating, particularly in the field of model updating of bridges based on experimental vibration data. In this specific research topic, the research of Cantieni et al. [17,21] and Zabel and Brehm [10] should be emphasized. Genetic algorithms have recognized advantages such as the non-dependence of the initial starting point, capability to manage a large number of parameters and constraints, possibility to handle with discrete and binary variables, ability to find the global minimum in functions with several local minima and the possibility to accept failed designs. On the other hand, a low convergence rate in comparison to gradient-based methods is generally agreed to be its main disadvantage.

This paper describes the finite element model updating of a bowstring-arch railway bridge based on experimental modal data.

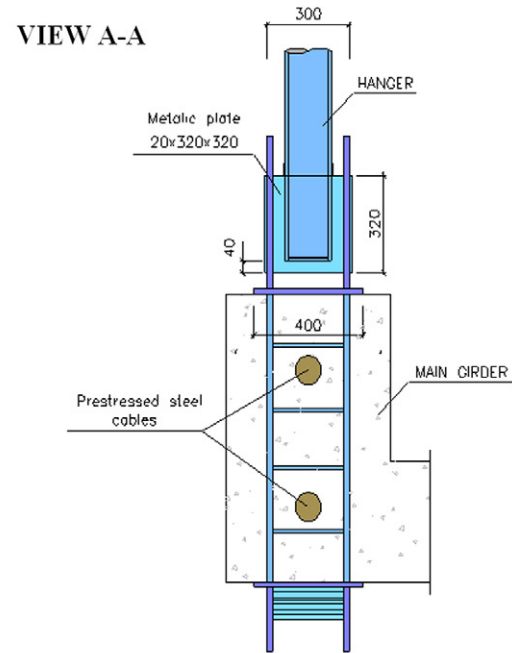
The detailed description of a three-dimensional FE model of the bridge is presented. The dynamic properties of the bridge are determined by an ambient vibration test that allows the identification of the natural frequencies, mode shapes and damping coefficients of the bridge. This experimental test is basically focused on the characterization of the overall dynamic behavior of the structure, in particular of the bridge deck and arches. Additionally, the local dynamic behavior of some elements of the arches is also studied. This local dynamic behavior gives important information to characterize the structural continuity between the deck and the arches. The calibration of the numerical model involves a sensitivity analysis and an optimization process. In the scope of the model calibration special emphasis is given to the application of an innovative mode pairing criteria based on modal strain energies [25]. This criterion uses the so-called energy-based modal assurance criteria (EMAC) to perform the correct pairing between the numerical and experimental mode shapes. The efficiency of this criterion, in comparison with the classical modal assurance criteria (MAC), is demonstrated. A global sensitivity analysis, based on a stochastic sampling strategy, is performed to identify the design parameters that influence the modal results and consequently may be used for updating the numerical model. The optimization is performed by means of an iterative procedure using a genetic algorithm. This phase is based on the minimization of an objective function that includes terms related to the residuals of the frequencies and mode shapes. These residuals include terms related to the global and local dynamic behavior of the bridge. The validation of the model is performed based on the results of an ultrasonic test for the confirmation of the modulus of deformability of the concrete and a dynamic test for the passage of railway traffic.

2. São Lourenço railway bridge

São Lourenço railway bridge is located at km +158.662 of the Northern line of the Portuguese railways that establishes the rail



(a)



(b)

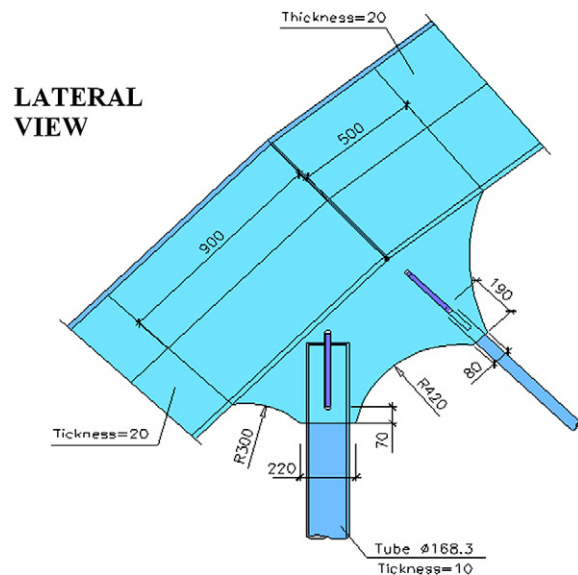


Fig. 2. Structural connections: (a) between hanger and girder, (b) between hanger and arch.

connection between Lisbon and Porto, in a recently upgraded section for the passage of trains which can travel at speeds up to 200 km/h.

The bridge is a bowstring arch consisting of two half-decks with 42 m span, each one carrying a single track. Each deck consists of a 0.40 m thick prestressed concrete slab suspended by two longitudinal arches. The suspension is performed by means of metallic hangers and diagonals. The arches are linked in the upper part by transversal girders that assure the bracing of the arches.

The deck is supported at each abutment by two pot bearings. The distance between the supports is 38.4 m, and the extremities of the deck slab work as cantilevers with 1.8 m span. Each half-deck cross section, with a total width of 7.35 m, consists of a concrete slab laterally supported by two main girders, forming a U-section, and

a side footway. In Fig. 1 a lateral view of São Lourenço bridge and a cross section of the deck are presented.

The arches are composed of several metallic parts with a welded rectangular box-section. Metallic hangers connected to the main girders perform the suspension of the deck. At both extremities the arches are connected to concrete blocks, by means of metallic plates and anchor bolts. The hangers are circular hollow sections with a diameter of 168.3 mm and a thickness of 10 mm. The diagonals are composed of two steel bars with a diameter of 50 mm.

Fig. 2 shows the details of the connections between the hanger and the main girder and between the hanger and the arch.

The connection of the hangers to the main girders is performed by means of metallic plates welded to the base of the hangers. These

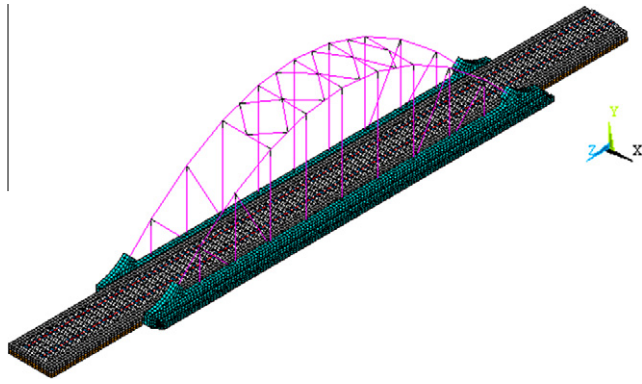


Fig. 3. Three-dimensional model of São Lourenço railway bridge including the track.

plates, connected at various levels with reinforcement plates, cross the girder and are anchored to its lower surface (Fig. 2a). The connection of the hangers to the arch is also performed through metallic plates welded to the top of the hangers according to the details presented in Fig. 2b.

3. Numerical modelling

3.1. Description

The dynamic analysis of São Lourenço railway bridge was performed using a three-dimensional model, including the track, developed in ANSYS® software [26]. A global view of the numerical model of the bridge is presented in Fig. 3.

The deck slab was modelled with solid elements. The arches, hangers, diagonals and bracings were modelled with beam elements. The track was modelled in an extension corresponding to the bridge length and in a distance of about 10 m from each abutment, in order to simulate the support of the track on the adjacent embankments. The rails were modelled by beam elements levelled with the center of gravity axis, and the sleepers and the ballast layer were modelled using solid finite elements. The connections related to the support bearings were located at their centers of rotation. The structure was divided into 16,979 solid elements and 1107 beam elements, with a total of 26,754 nodes and 80,029 degrees-of-freedom.

For modelling the structure, particular attention was given to the connection between the ends of the arches and the support blocks to guarantee a monolithic link. As the solid finite elements

Table 1
Characterization of the parameters of the numerical model of São Lourenço bridge.

Parameter	Designation	Statistical properties		Limits (lower/upper)	Adopted value	Unit	References		
		Distribution type	Mean value/standard deviation						
E_c	Modulus deformability concrete	Normal	38.7/3.87	31.0/46.4	38.7	GPa	[27–29]		
ρ_c	Density concrete	Normal	2446.5/97.9	2286/2607	2446.5	kg/m ³	[30,31]		
ν_c	Poisson ratio concrete	–	–/–	–/–	0.20	–	[32]		
E_{bal}	Modulus deformability ballast	–	–/–	–/–	130	MPa	[33]		
ρ_{bal}	Density ballast	Uniform	1885/147.2	1630/2140	1733	kg/m ³	[10,30,34]		
ν_{bal}	Poisson ratio ballast	–	–/–	–/–	0.20	–	[32]		
E_s	Modulus deformability steel	Normal	202/8.1	188.7/215.3	202	GPa	[35]		
ρ_s	Density steel	–	–/–	–/–	7850	kg/m ³	[32]		
ν_s	Poisson ratio steel	–	–/–	–/–	0.30	–			
K_v	Vertical stiffness of the supports	Log-normal	7419/6929	–/–	3847	MN/m	–		
K_{palm}	Vertical stiffness of the rail pads	–	–/–	–/–	400	MN/m	[36]		
A_{rail}/I_{rail}	Area/inertia of rail UIC 54	–	–/–	–/–	69.3/2346	cm ² /cm ⁴	[37]		
A_{arch}/I_{arch}	Area/inertia of arch (current section)	–	–/–	–/–	374.4/275,700	cm ² /cm ⁴	[38]		
A_H/I_H	Area/inertia of hangers	–	–/–	–/–	49.7/1560	cm ² /cm ⁴			
A_{diag}/I_{diag}	Area/inertia of diagonals	–	–/–	–/–	39.3/61.4	cm ² /cm ⁴			
I_{diag}^l	Inertia of the connection	Diagonal-deck and diagonal-arch	Axle x ^a	Uniform	3101/1754.7	61.4/6140	500	cm ⁴	
I_{diag}^t			Axle z ^a						
I_H^l		Hanger-deck and hanger-arch	Axle x ^a	Uniform	3125/903.6	1560/4690	2000	cm ⁴	
I_H^t			Axle z ^a		16,420/8579.4	1560/31,280			
σ_0^{DLE1}	Initial stress	DL ^b outer 1		Uniform	37.5/21.7	0/75	0	MPa	–
σ_0^{DLE2}		DL ^b outer 2							
σ_0^{DLI1}		DL ^b inner 1							
σ_0^{DLI2}		DL ^b inner 2							
σ_0^H		H							
σ_0^{DSE}	DS ^b outer			Uniform	100/28.9	50/150	0	MPa	

^a The axles are according to the cartesian referential presented in Fig. 3.

^b DL – diagonal longer; DS – diagonal shorter; H – hangers.

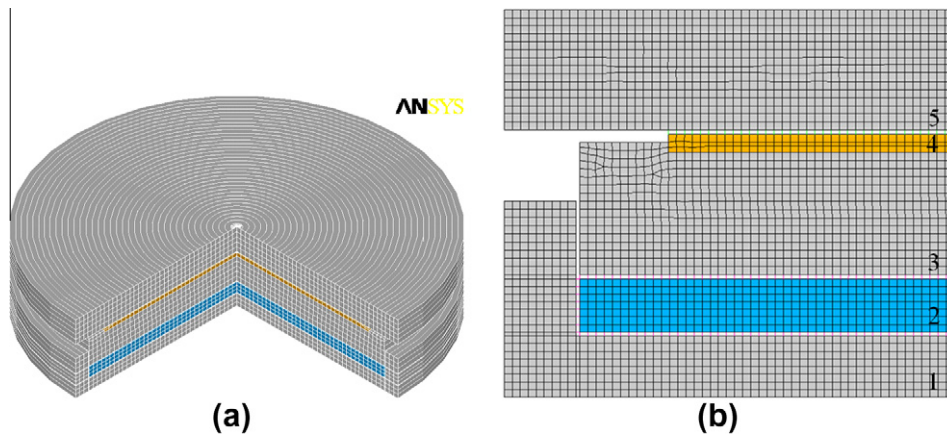


Fig. 4. Numerical model of the support: (a) general view; (b) detail.

Table 2

Characterization of the parameters of the numerical model of the support.

Parameter	Designation	Statistical properties		Adopted value	Unit	References
		Distribution type	Limits (lower/upper)			
E_{rub}	Modulus deformability rubber	Uniform	10/100	50	MPa	[39,40]
ν_{rub}	Poisson ratio rubber		0.47/0.4999	0.48		[41–43]
μ_{st-rub}	Friction coefficient steel-rubber		0.005/0.20	0.10		[39]
E_{tef}	Modulus deformability Teflon		600/700	650	–	[44]
ν_{tef}	Poisson ratio Teflon		0.44/0.47	0.46		[44,45]
μ_{st-tef}	Friction coefficient steel-Teflon		0.06/0.10	0.07		[44]

of the support blocks do not have rotational degrees of freedom, the beam elements of the arch were extended inside the solid elements in order to guarantee the continuity of the rotations in these connections. Identical procedure was adopted for the connections between the hangers and diagonals with the deck slab.

To correctly reproduce the deformability length of the hangers and diagonals, rigid elements were introduced in the extremities of the beam elements.

3.2. Geometrical and mechanical properties

Table 1 describes the geometric and mechanical parameters of the numerical model of the bridge, including its designation, the adopted value and the respective unit and some references. Additionally, the statistical properties of some of the parameters that will be used later in the model calibration phase are listed. The lower and upper limits of the normal statistical distributions were obtained by subtracting or adding to the average value, a value equal to two times the standard deviation.

Due to the inexistence of information in the project about the vertical stiffness of the supports, the evaluation of this parameter was based on the FE numerical model presented in Fig. 4. The model includes the metallic pot (1), the elastomeric rubber pad (2), the piston (3), the Teflon layer (4) and the upper metallic plate (5). All components were modelled by finite elements in axisymmetric conditions, with exception of the interfaces between rubber-steel and Teflon-steel that were modelled by Coulomb friction elements with a resistance dependent of the normal load on sliding surface.

In Table 2 several parameters of the numerical model of the support are characterized with the indication of the adopted values and respective units. The lower and upper limits for each parameter and some references are also presented.

The vertical stiffness of the support was calculated considering the adopted values of the parameters listed in Table 2, by dividing the force in correspondence to the application of a unit uniformly

distributed vertical load in the upper plate for the average displacement of the plate, resulting 3847 MN/m.

The characterization of the statistical distribution of the vertical stiffness of the support was based on a stochastic sampling technique, using the Latin Hypercube method [46,47], and considering the uniform distributions indicated in Table 2. The distribution of the vertical stiffness of the support, based on 750 samples, proved to be particularly sensitive to changes in the modulus of deformability and Poisson's ratio of the rubber. The distribution of the samples was adjusted by means of a log-normal probability density function with an average value equal to 0.7419×10^4 MN/m and a standard deviation equal to 0.6929×10^4 MN/m.

The dynamic behavior of the diagonals and hangers is significantly influenced by the stresses on these elements, which are derived not only from the permanent loads of the structure, but also from the construction stage and the temperature variations. The parameters σ_0 take into account the possible variations of the stresses installed in these elements.

The masses of non-structural elements such as coatings, lateral parapets, and footway slabs were calculated and added on the nodes of the finite element mesh in correspondence with the locations of each of those elements.

3.3. Modal parameters

The natural frequencies of São Lourenço bridge are associated with different types of modes of vibration, namely global modes (G) and local modes (L).

The global modes involve global modal deflections of the bridge deck or arches. The local modes are associated with local vibrations of diagonals and hangers, with no significant modal deflections of the deck or arches. Some global modes are coupled with local modes. These particular modes are characterized by common movements, with similar amplitude, of the deck or arches with the diagonals or hangers. The modal analysis of the bridge was

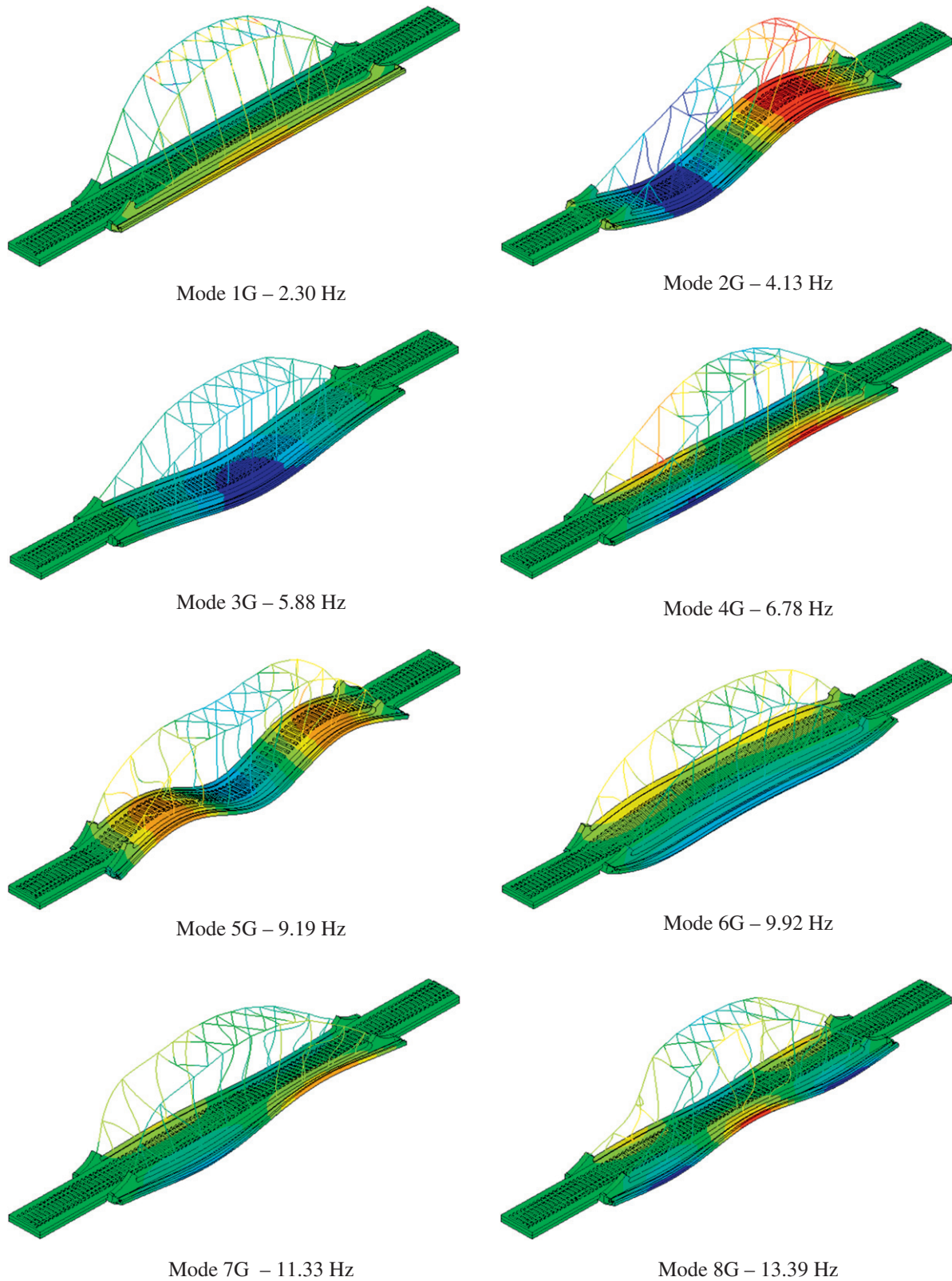


Fig. 5. Numerical global natural frequencies and mode shapes.

performed considering the stress stiffening due to the permanent loads.

In Fig. 5 the natural frequencies of the most relevant calculated global modes of the bridge and the corresponding mode shapes are presented. Modes 1G, 4G and 8G essentially involve the transversal

bending of the arches. Modes 2G, 3G, 5G, 9G and 11G are flexural modes of the deck; on the other hand, modes 6G, 7G, 10G and 12G are torsional modes of the deck.

Fig. 6 shows the values of the natural frequencies and mode shapes of some of the local modes mainly associated with modal

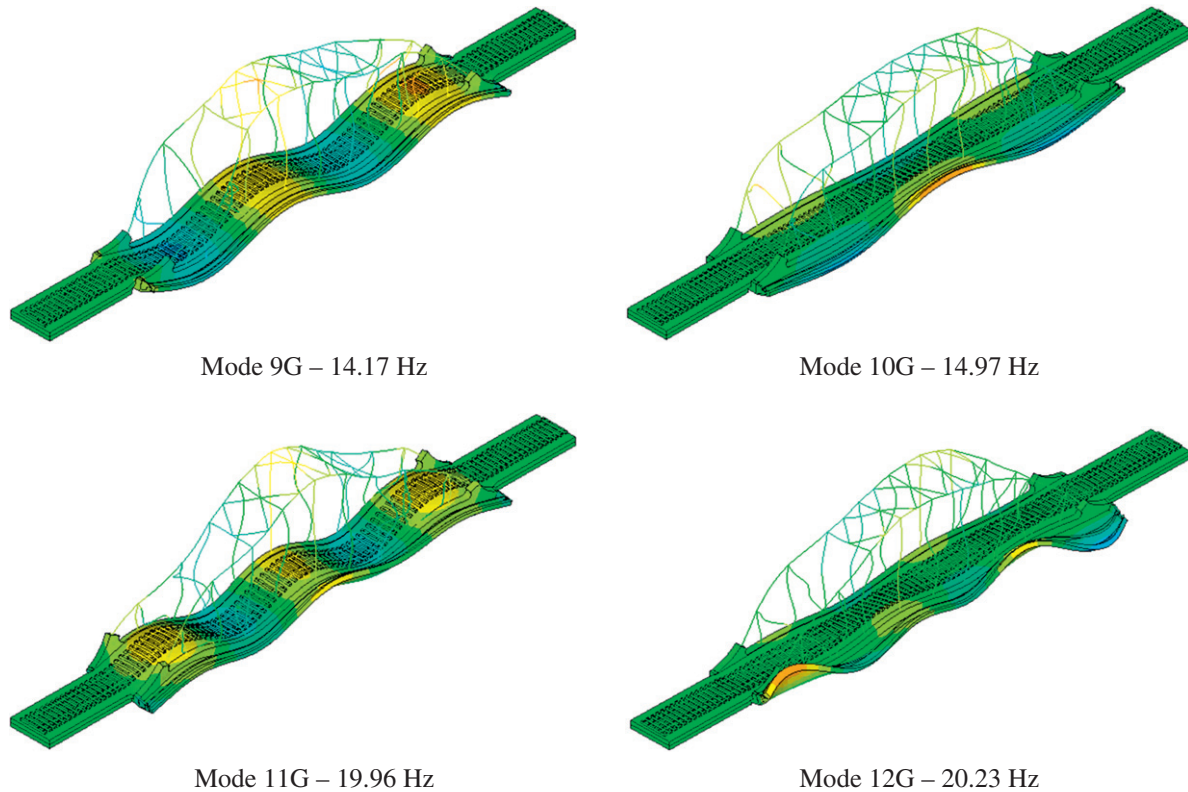


Fig. 5 (continued)

deflections of the longer diagonals (DL), shorter diagonals (DS), and the hangers located at mid-span of the deck (H). It should be noted that in the figure are only represented the modes of the elements for which sensors were placed in the ambient vibration test (see Section 4). For a better visualization only the deformed shape of the arches (3D view and lateral view) are represented, attending that the modal deflections of the deck are negligible.

4. Ambient vibration test

4.1. Description

The ambient vibration test enabled to identify the modal properties of the bridge, namely, the natural frequencies, the mode shapes and the damping coefficients. This test was implemented using a technique that considers fixed reference points and mobile measuring points and involved the use of 12 piezoelectric accelerometers model PCB[®] 393A03. The ambient response was evaluated in terms of accelerations in the vertical, transverse and longitudinal directions, in successive setups in a total of 55 measurement points located on the main girders of the deck, on the footway cantilever, on the arches and in some hangers and diagonals (Fig. 7). The reference sensors were located in the sections between 1/3 and 1/4 span of the deck (positions 11, 12, 23 and 24).

The data acquisition was performed using the cDAQ-9172[®] system from National Instruments, equipped with IEPE analog input modules with 24-bit resolution (NI 9233[®]). The acceleration series were acquired over periods of 10 min, with a sampling frequency of 2000 Hz and decimated to a frequency of 100 Hz.

The connection of the accelerometers to the girders of the deck was performed by means of metallic plates bonded to the surface of the concrete. The connection of the accelerometers to the elements of the arches was performed with plates fixed by means

of magnetic bases, in the case of the arch, or through clamped metallic double angles, in the case of the hangers and diagonals. The details of these connections are shown in Fig. 8. The installation of sensors in the arches was limited to a height of 2.80 m, with respect to the level of the footway, in order to satisfy the safety distance to the catenary.

Due to the reduced acceleration levels of the bridge under ambient conditions, a random external excitation was provided, in time and space, by means of a group of people jumping in several locations of the deck. This technique guarantees higher signal-to-noise ratios and consequently an increase of the coherence between the measured signals.

4.2. Modal parameters identification

4.2.1. Natural frequencies and mode shapes

The identification of the frequencies and modes of vibration of the bridge was performed by the application of the Enhanced Frequency Domain Decomposition method (EFDD) available in the software ARTeMIS[®] [48]. Fig. 9 shows the curves of the average normalized singular values of the spectral density matrices of all experimental setups.

The marked peaks correspond to global modes, coupled and uncoupled, and local modes of the bridge.

The local modes refer to the elements of the arches where the sensors were installed. The local modes of the longer diagonals, the most flexible elements of the arches have frequencies equal to 6.82, 7.76, 6.98, 8.59, 7.48, 9.09 and 8.24 Hz in correspondence with modes 1L to 7L. The modes of the mid-span hangers of the arches have frequencies equal to 11.64, 11.93 and 10.48 Hz, in correspondence with modes 8L to 10L. The modes of the shorter diagonals of the outer arch have frequencies equal to 18.86 and 19.23 Hz and correspond to modes 11L and 12L respectively.

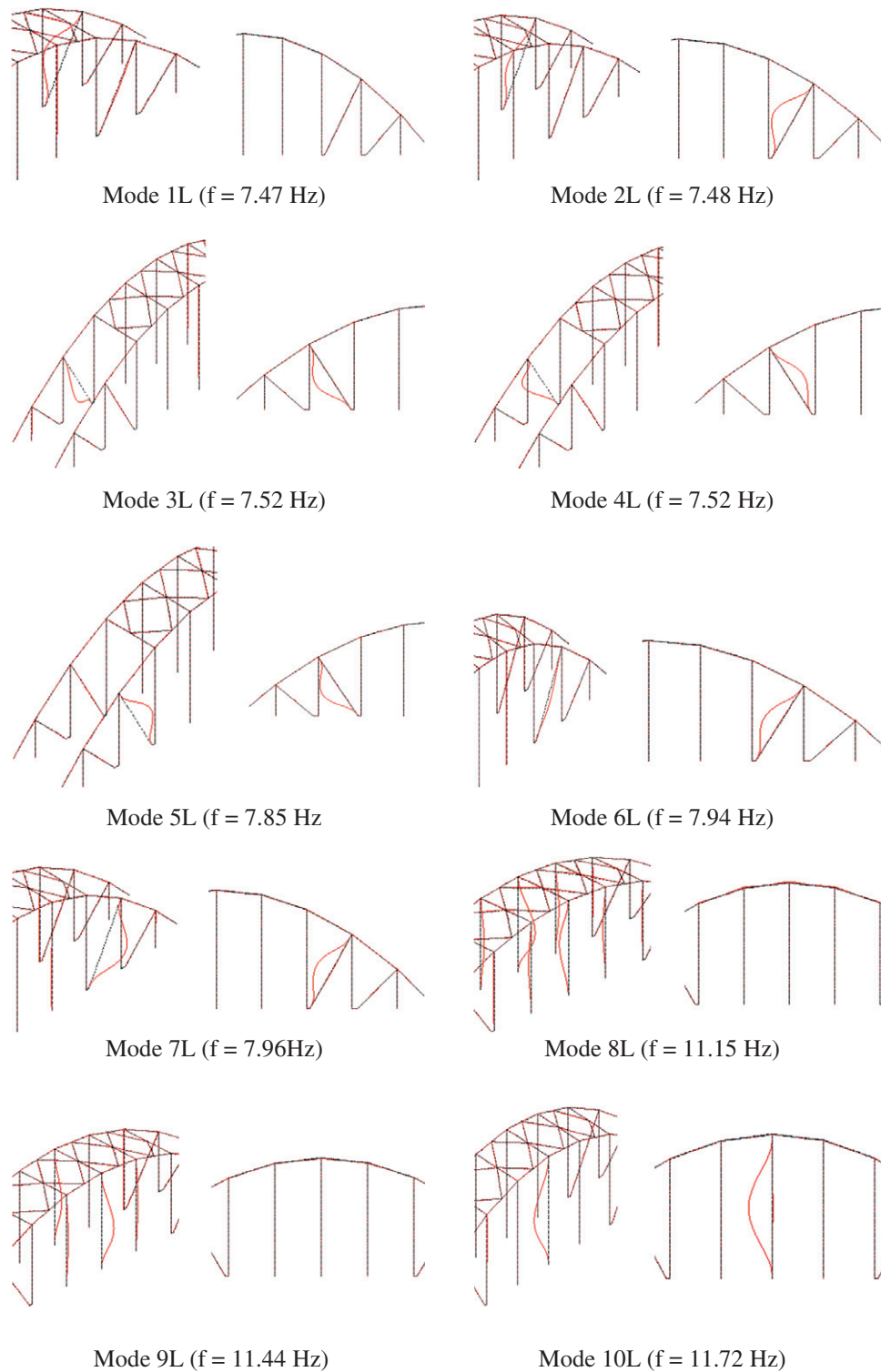


Fig. 6. Numerical local natural frequencies and mode shapes.

Fig. 10 illustrates the configurations of the identified global modes of vibration, indicating the respective frequencies. For a better understanding of the configuration of each mode, only the modal deflections of the main girders of the deck are represented.

Fig. 11 shows the values of the autoMAC correlation matrix of the experimental mode shapes obtained by the application of the EFDD method, and considering only the modal information of the

deck (Fig. 11a) and the modal information from the deck and arches (Fig. 11b).

The observation of the figure shows significant correlations between the pairs of modes 1G-6G, 4G-7G and 8G-10G, because of the similarity between the configurations of these modes when considering only the modal information of the deck. The measurement points located at the arches, diagonals and hangers allowed

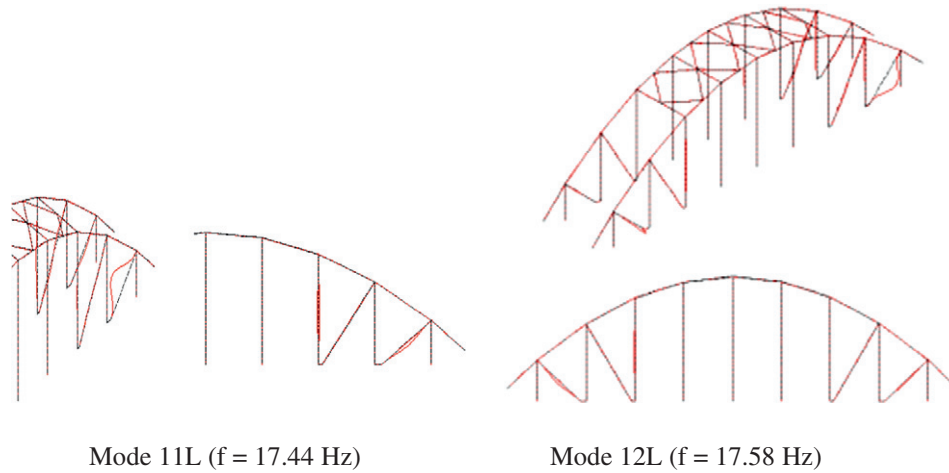


Fig. 6 (continued)

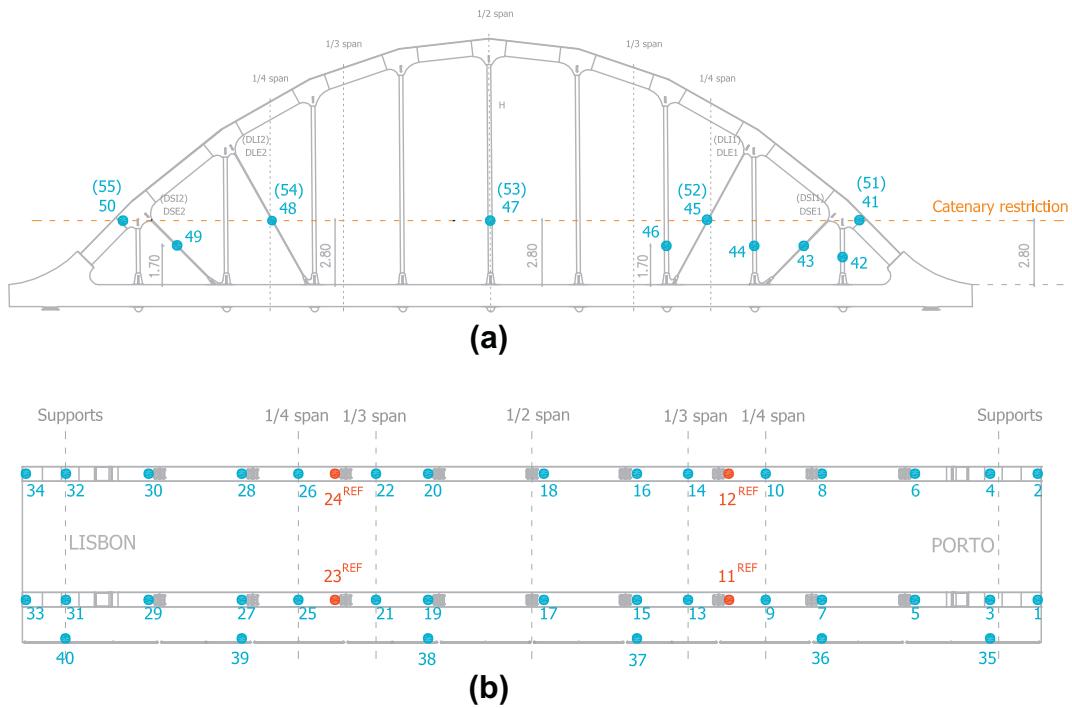


Fig. 7. Measuring points of the ambient vibration test: (a) arches and (b) deck.

scaling the modal deflections of the deck, in order to correctly assess the nature of the modes.

4.2.2. Damping coefficients

Fig. 12 presents the damping coefficients estimates obtained by EFDD method for the different experimental setups. The estimates of damping coefficients of the global modes show an overall decrease with the increase of the frequency of vibration. Mode 2G shows the highest damping values, between 1.15% and 1.60%, and also the highest dispersion of results. Modes 1G, 3G and 4G have damping coefficients between 0.50% and 1.00%, and the remaining global modes have damping values lower than 0.50%. The damping coefficients of the local modes have lower dispersion and are generally located between 0.10% and 0.30%.

5. Calibration of the numerical model

The calibration of the numerical model of the bridge was based on the results of the ambient vibration test and involved two stages: a sensitivity analysis and an optimization process. The technique adopted for the mode pairing between numerical and experimental modes of vibration is also discussed.

5.1. Mode pairing criteria

The mode pairing technique establishes the correspondence between each experimentally obtained mode and a numerically derived mode. Brehm et al. [25] stressed that a correct assignment is important to assure a correct sensitivity analysis and a well-shaped objective function applied in the optimization-based model

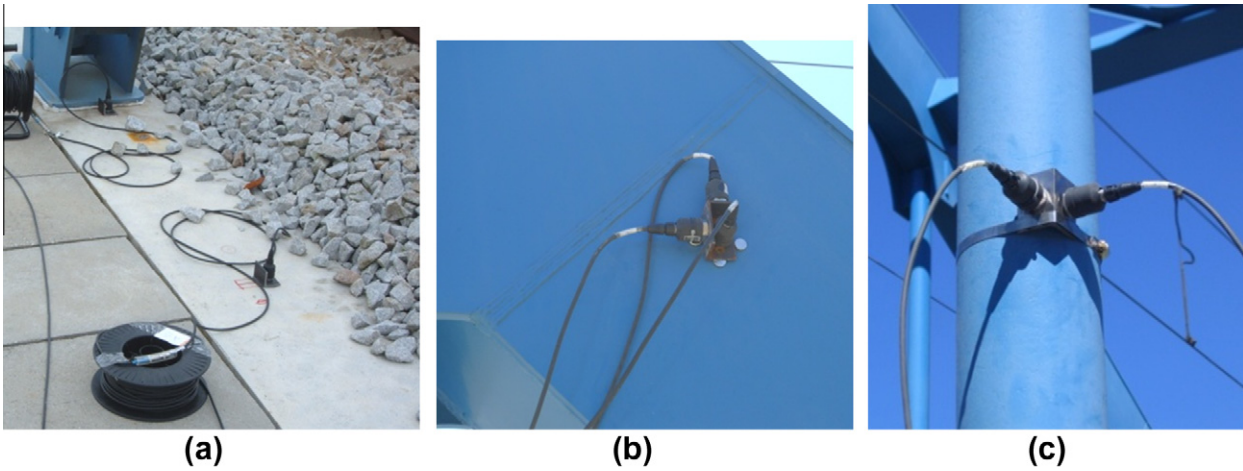


Fig. 8. Installation of the accelerometers: (a) deck, (b) start of the arch and (c) hanger.

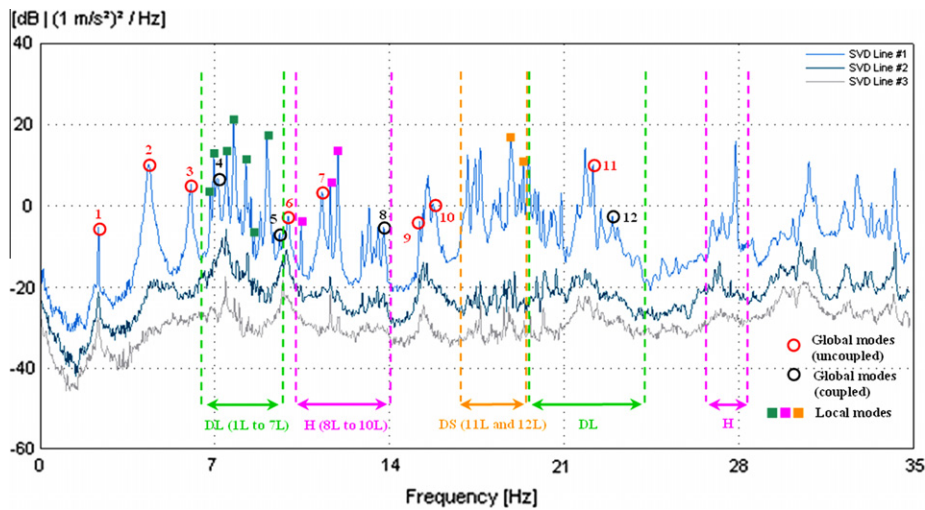


Fig. 9. EFDD method: average normalized singular values of the spectral density matrices.

updating. However, the definition of a stable pairing criterion is a complex task due to the usually limited number of measurement points. Additionally, changes of the updating parameters can lead to switches of modes with close frequencies.

In this paper, the energy-based modal assurance criterion

$$EMAC_{ijk} = \prod_{jk} MAC_{ij} \quad (1)$$

proposed by Brehm et al. [25], has been applied. This criterion enhances the traditional modal assurance criterion MAC [49]

$$MAC_{ij} = \frac{(\widehat{\Phi}_i^T \widehat{\Phi}_j)^2}{(\widehat{\Phi}_i^T \widehat{\Phi}_i)(\widehat{\Phi}_j^T \widehat{\Phi}_j)} \quad (2)$$

by the relative modal strain energy (Π_{jk}) of a certain cluster k of numerical degrees-of-freedom related to a numerical mode j , where $\widehat{\Phi}_j$ is the numerically derived vector containing the coordinates of the numerical mode j corresponding to the experimental degrees-of-freedom and $\widehat{\Phi}_i$ is the experimentally obtained vector containing the experimental information of mode i . The clusters k should reflect the information extracted from the distribution of

measurement points and their measurement directions related to a specific mode. Further discussions were presented in Refs. [14,25].

In this specific application, the clusters are related to the translational degrees-of-freedom of the six element groups indicated in Fig. 13. The other elements cluster contains all remaining degrees-of-freedom, such as, the remaining rotational degrees-of-freedom of all element groups and the translational degrees-of-freedom in y direction of the hangers $\frac{1}{2}$ span.

Fig. 14 shows the values of the relative modal strain energy of each cluster related to all numerical modes in the range between 2.3 and 29.4 Hz of the initial finite element model.

The global modes are associated with higher energy values of the clusters deck and arches. The local modes have higher energy values in the clusters diagonals and hangers $\frac{1}{2}$ span. Therefore, the EMAC related to the global modes 1G to 4G, 7G and 9G are based on a joint cluster of deck and arches, while for the remaining global modes only the relative modal strain energy of the deck cluster is considered. Depending on the involved elements in each particular local mode, the clusters diagonals and/or hangers $\frac{1}{2}$ span are applied to calculate the EMAC value. The cluster footway was not useful at all for the mode pairing.

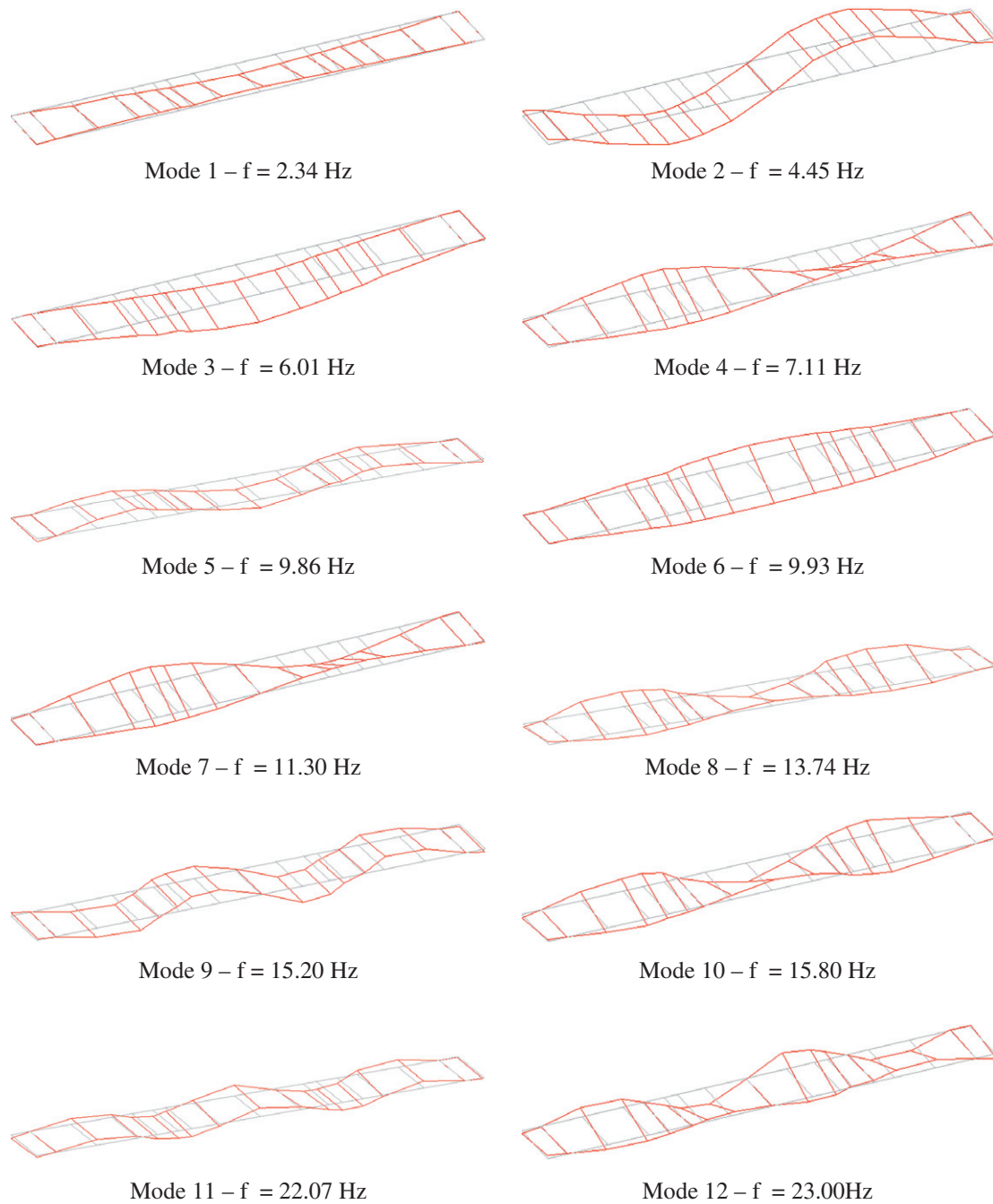


Fig. 10. Experimental global natural frequencies and mode shapes.

Fig. 15a and b illustrate the MAC and EMAC matrices between experimental and numerical modes of the initial finite element model, respectively. For a simple visualization, each matrix is divided into two submatrices, referring to the global and local modes. Using these matrices, the most likely numerical mode can be assigned to each experimental mode, which is indicated by the highest value in each row. Of course, the final paired modes can be different, whether the MAC or EMAC is applied as mode assignment criteria. For this specific input parameter set, the correct mode pairing can be determined by visual inspection. These results can be used to assess the ability of both criteria to find the most likely mode pairing.

In general, the EMAC is more reliable for the detection of the correct mode pairing than the simple MAC criterion. This can be,

for example, observed for the experimental mode 6G. The MAC is assigning the 9th numerical mode, which is mainly characterized by the simultaneous vibration of the two longer diagonals of the outer arch. The modal torsional deflection of the main structure is of minor order in this mode. Therefore, the wrong mode would be assigned if using the MAC criterion. Based on the EMAC parameter, a correspondence between the experimental mode 6G and the correct numerical mode 15 was established. This numerical mode essentially mobilizes the modal energy of the deck. Concerning the local modes, it is important to emphasize the importance of the EMAC parameter for the correct pairing of modes 8L and 11L. To improve the efficiency of the pairing of modes 1L and 7L in addition to the adoption of EMAC values, frequency limits were imposed to avoid pairing with higher order modes. For example

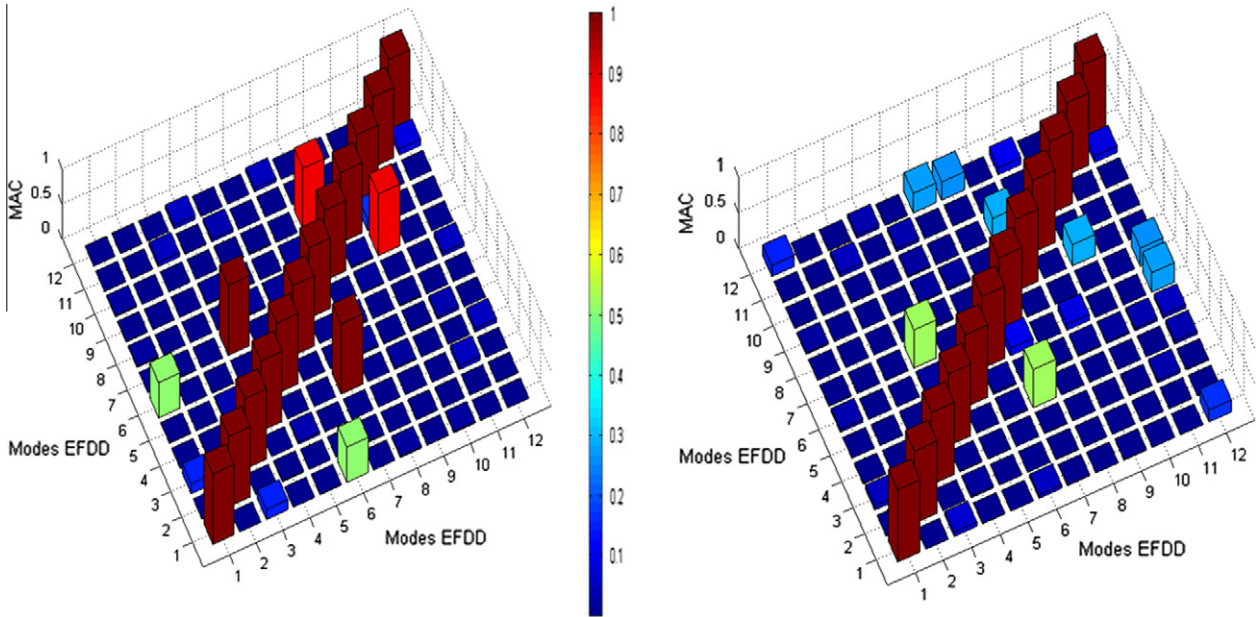


Fig. 11. AutoMAC correlation matrix of the experimental modes shapes obtained by the application of the EFDD method, and considering only the modal information of the: (a) deck (b) deck and arches.

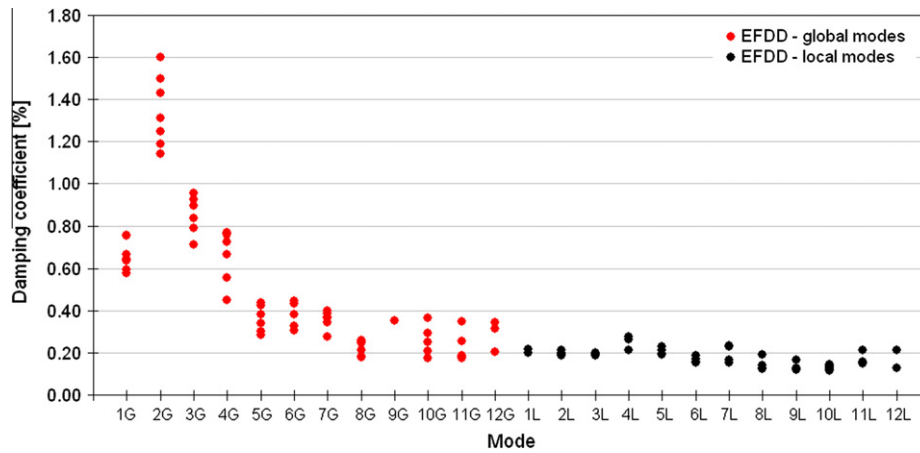


Fig. 12. Damping coefficients estimated by EFDD method for the different experimental setups.

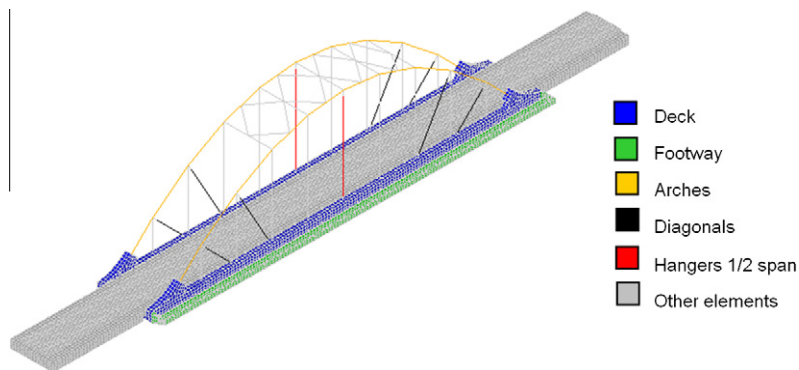


Fig. 13. Clusters used in the mode pairing.

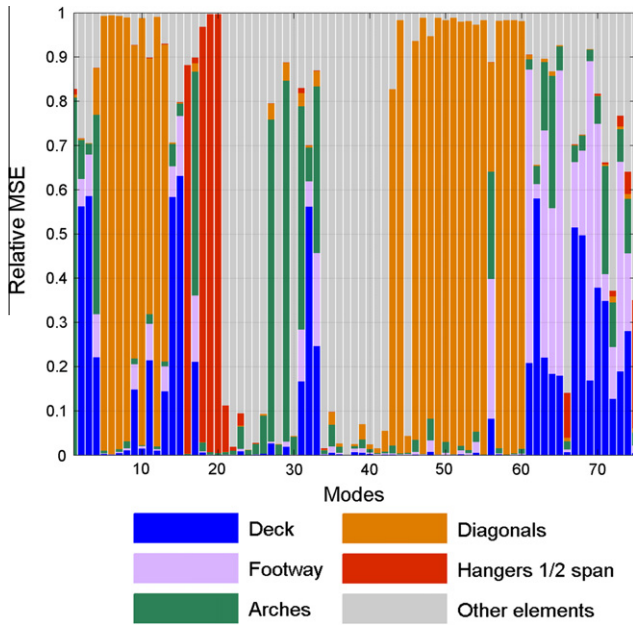


Fig. 14. Relative modal strain energy of each mode based on the initial FE model of the bridge.

in the case of experimental mode 3L, which tends to pair with the numerical mode 55 based on the MAC value, is paired with the numerical mode 7 using the EMAC value and the frequency restrictions.

5.2. Sensitivity analysis

The sensitivity analysis allows for the selection of the parameters that most influence the frequencies and MAC values of the global and local modes, and consequently should be included in the subsequent optimization phase. In contrast to sensitivity analyses, in which only one parameter is varied at one time (e.g., Saltelli et al. [50]), all uncertain input parameters are varied simultaneously in this study. This has the advantage of obtaining global sensitivities for all pairs of parameters with a single sample set. The multivariate samples are generated by a stochastic sampling technique, the Latin hypercube sampling, which outperforms traditional design-of-experiment sampling schemes, such as the full factorial design. The samples are related to a multivariate uniform distribution with the limits given in Table 1. The automatic mode pairing criteria, based on the EMAC, was crucial for the correct identification of the most suitable set of parameters.

Fig. 16 shows the results of a global sensitivity analysis through a Spearman linear correlation matrix [25]. The sensitivity analysis was based on 750 Latin hypercube samples. The samples related to

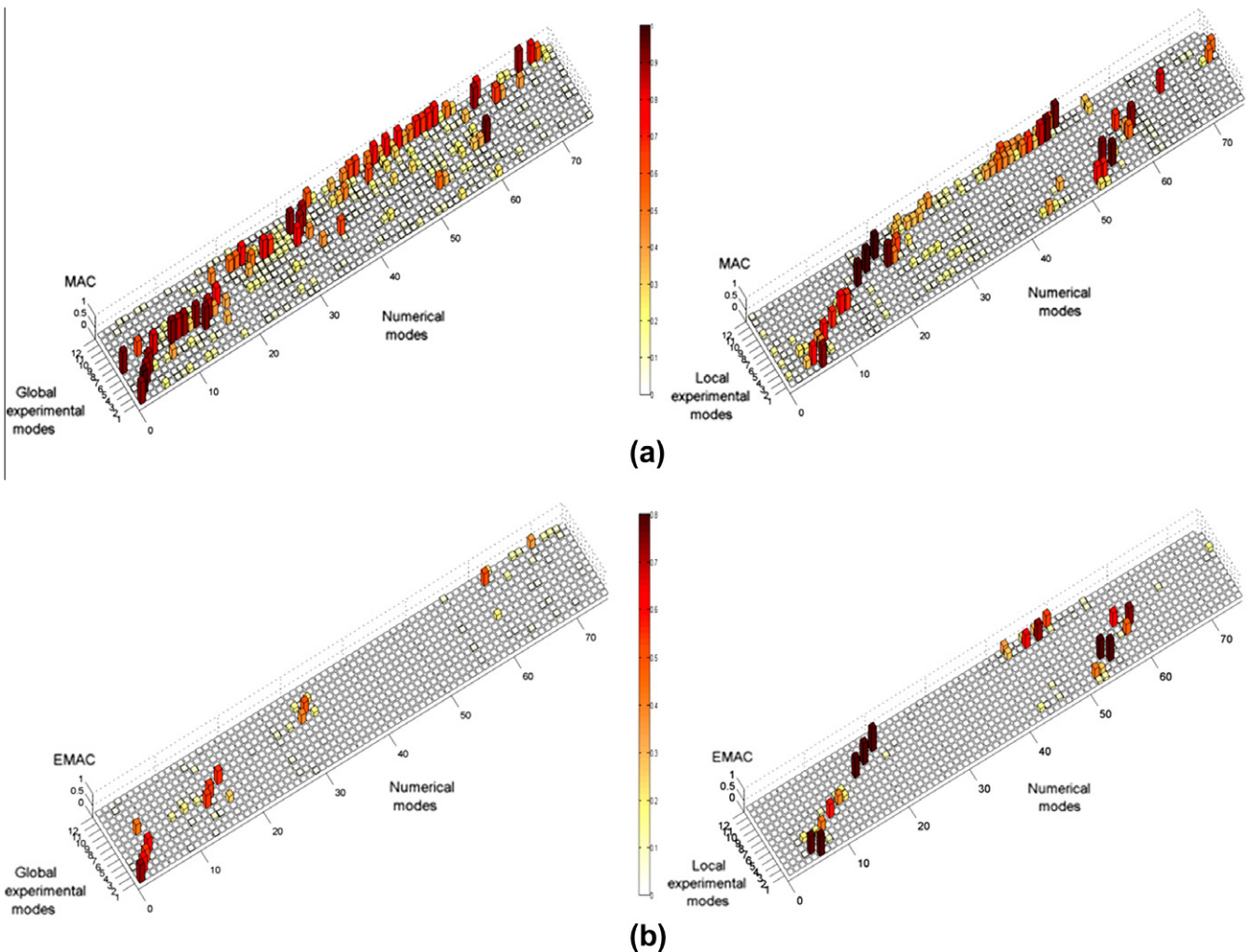


Fig. 15. (a) Modal assurance criterion (MAC) between numerically derived and experimentally obtained modes shapes, (b) energy-based modal assurance criterion (EMAC) between numerically derived and experimentally obtained modes shapes.

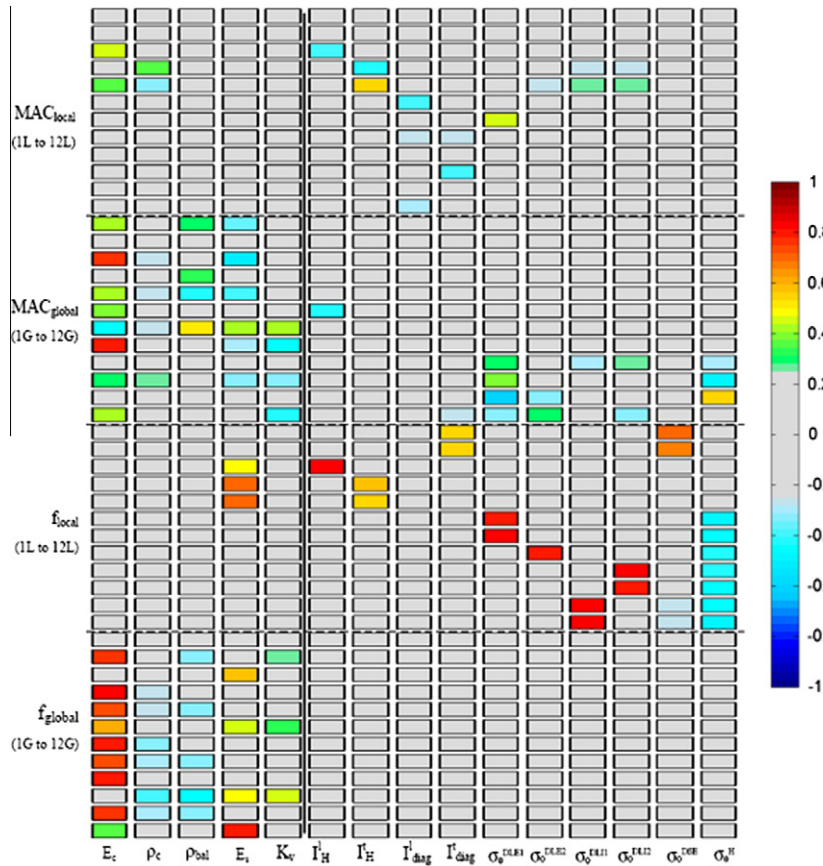


Fig. 16. Spearman correlation matrix between the parameters and the responses of the numerical model of the bridge.

a MAC value below 0.50 were removed. The correlation coefficients located in the interval $[-0.25; 0.25]$ were excluded from the graphical representation.

The correlation matrix shows that the modulus of deformability of concrete and steel, the density of concrete, the density of ballast and the vertical stiffness of supports have a significant influence on the frequencies and MAC values of the global modes. Furthermore, the parameters associated with the initial stress of the hangers and diagonals and the stiffness of the connections between these elements and the deck and arches have an important influence on the frequencies and MAC values of the local modes. All the analyzed numerical parameters revealed important sensitivities and consequently will be used in the optimization process.

5.3. Optimization

The optimization phase allowed obtaining the parameter values that minimize the differences between the numerical and experimental modal responses, and involved the definition of an objective function and the application of an optimization technique based on a genetic algorithm.

Fig. 17 presents a flowchart that illustrates the iterative process of calibration of the numerical model. The process involves the use of three software packages: ANSYS® [26] MATLAB® [51] and OptiSlang® [52].

In ANSYS® environment the FE numerical model is developed based on a set of initial parameter values, and the mass and stiffness matrices are extracted. In MATLAB® software, the eigenvalues and eigenvectors problem is solved, and based on the experimental modal information, the mode pairing between numerical and experimental modes using the EMAC is performed. The values of

the natural frequencies and MAC values are exported in text format. Finally, the OptiSlang® software, based on an objective function and on the application of an optimization technique supported by a genetic algorithm, estimates a new set of parameters focused on the minimization of the objective function residuals. This procedure is repeated iteratively until the maximum number of generations is reached.

The objective function (f) comprises two terms, one related to the natural frequencies of global and local modes, and another related to the MAC values of global and local modes:

$$f = a \sum_{i=1}^{nmodes} \frac{|f_i^{exp} - f_i^{num}|}{f_i^{exp}} + b \sum_{i=1}^{nmodes} |MAC(\phi_i^{exp}, \phi_i^{num}) - 1| \quad (3)$$

where f_i^{exp} and f_i^{num} are the experimental and numerical frequencies for mode i , ϕ_i^{exp} and ϕ_i^{num} are the vectors containing the experimental and numerical modal information regarding the mode i , a and b are weighing factors of the terms of the objective function, assumed in this case equal to 1.0, and $nmodes$ is the total number of modes equal to 24.

The optimization of the bridge model involved the use of 15 design variables and 48 modal responses. The genetic algorithm was based on an initial population consisting of 30 individuals and 150 generations, for a total of 4500 individuals. The initial population was randomly generated by Latin Hypercube method. In this algorithm the number of elites was equal to 1 and the number of substitute individuals was also defined equal to 1. The crossing rate was considered equal to 50% and the mutation rate was set equal to 15% with a standard deviation, variable along the optimization, between 0.10 and 0.01.

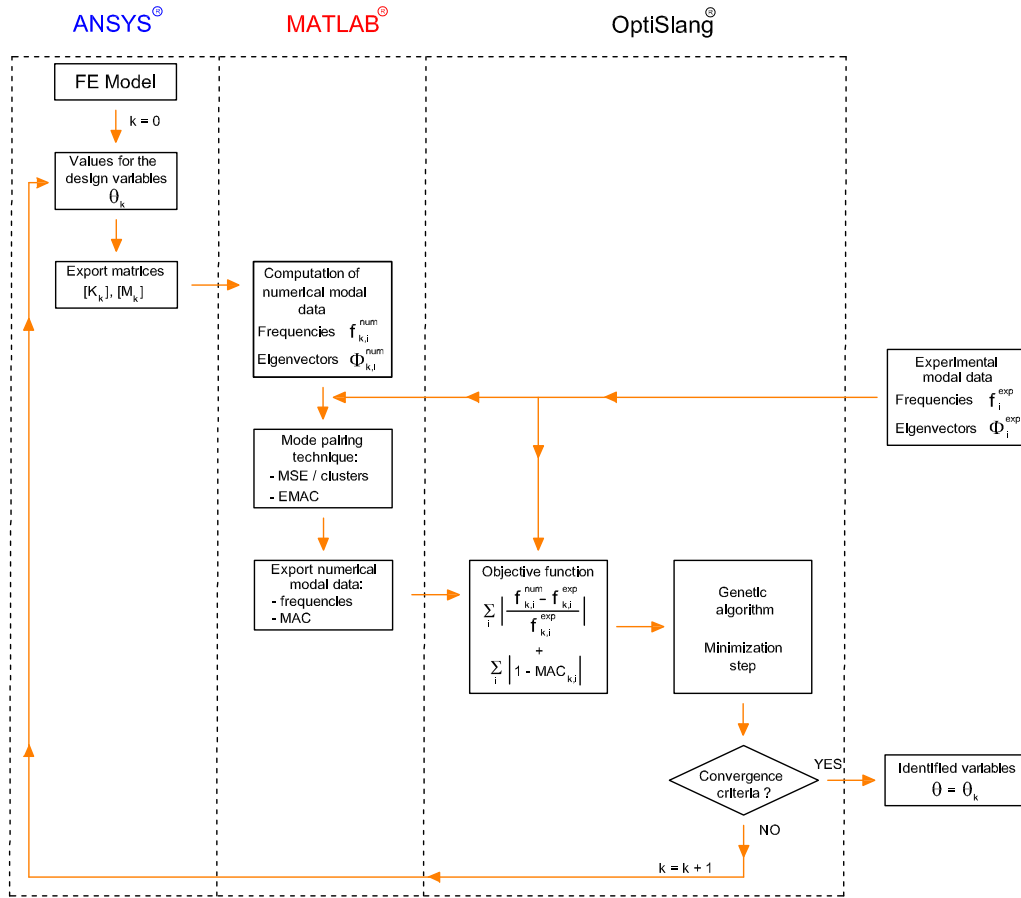


Fig. 17. Fluxogram of the optimization process of the numerical model.

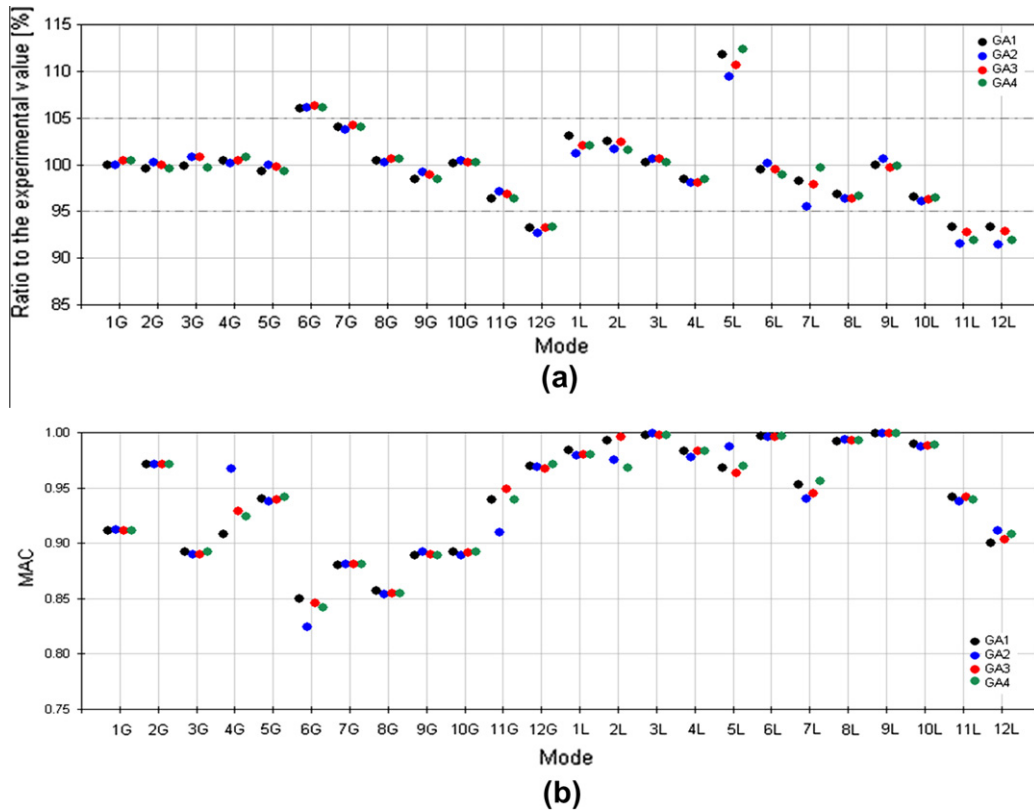
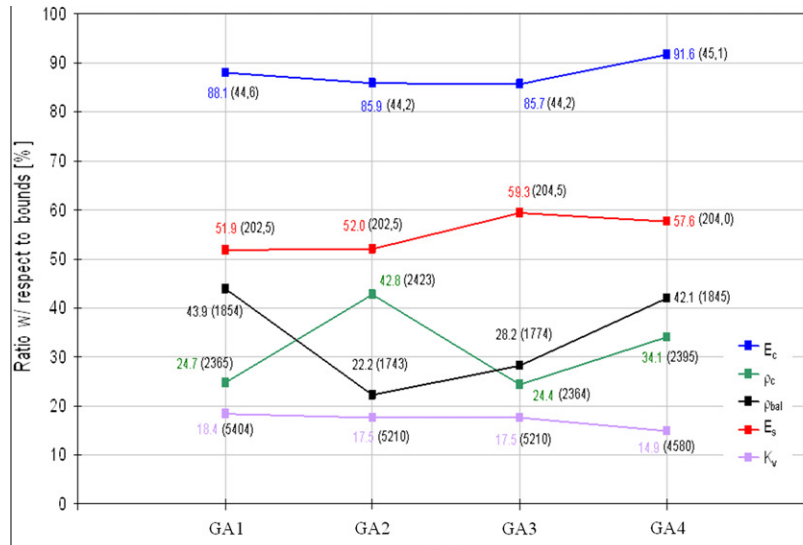
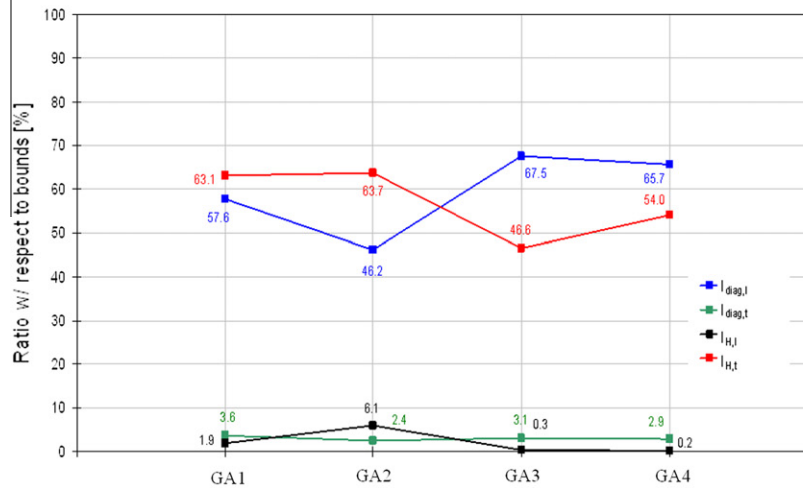


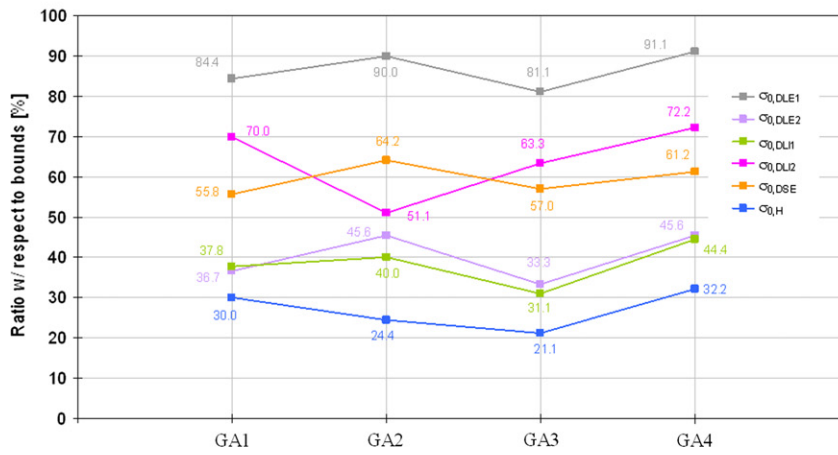
Fig. 18. Response values for the independent optimization runs GA1 to GA4: (a) natural frequencies and (b) MAC.



(a)



(b)



(c)

Fig. 19. Values of the numerical parameters for the optimization runs GA1–GA4: (a) global, (b) inertias of the connections between arch elements and deck and (c) initial stress on the diagonals and hangers.

The optimal values of the parameters were obtained based on the results of four independent optimization runs (GA1–GA4) with

different initial populations. The computational time spent in the calculation of each individual was approximately 105 s, on a

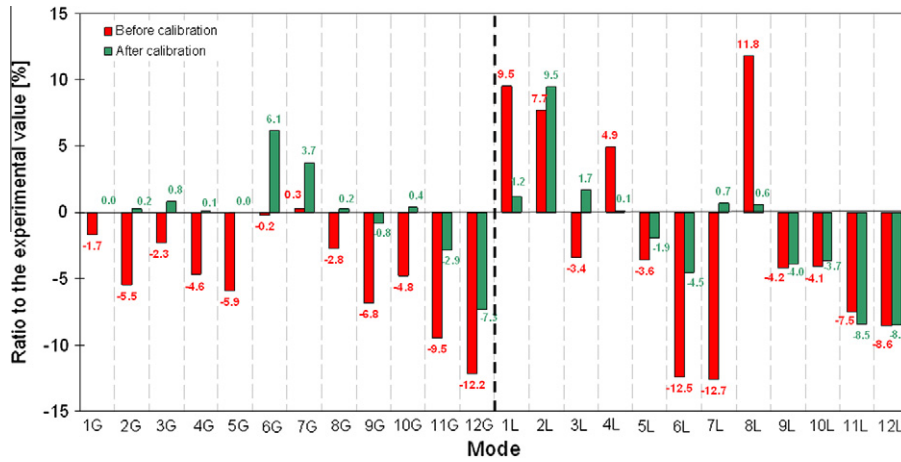


Fig. 20. Errors between the numerical frequencies, before and after updating, in relation to the average value of the experimental frequencies.

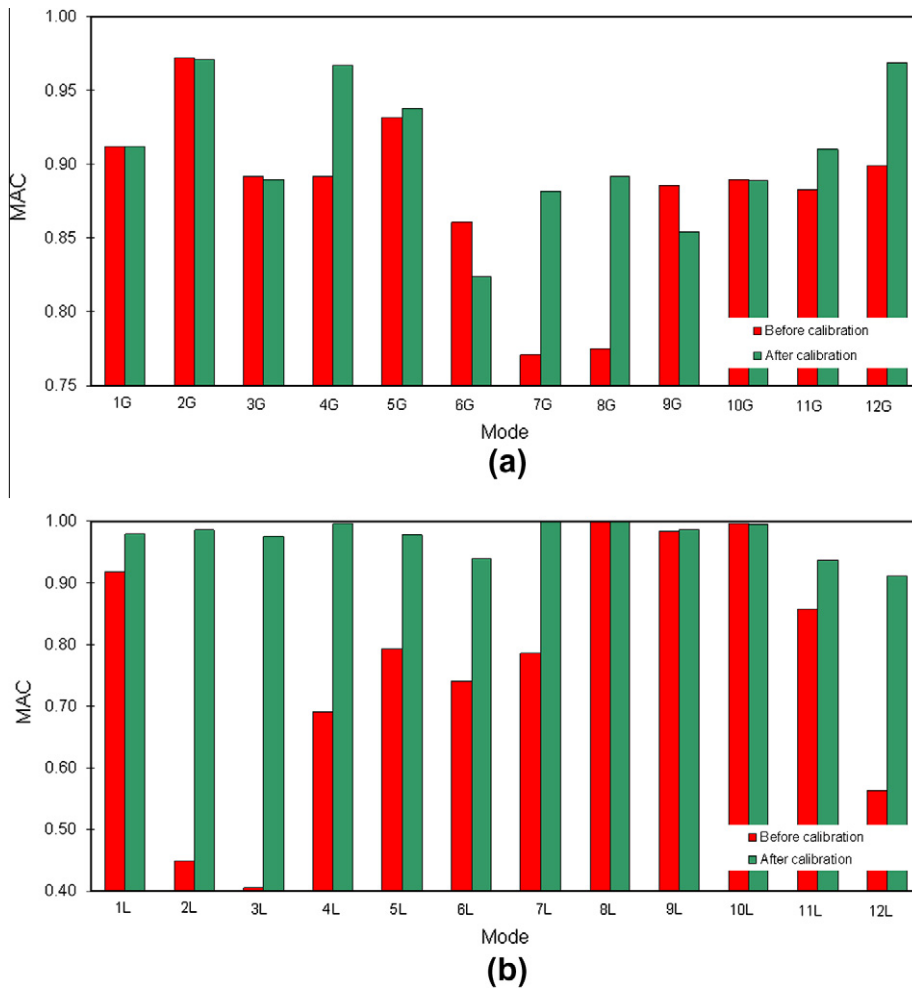


Fig. 21. Comparison of the MAC values, before and after the updating of the numerical model.

computer with two processors Intel® XEON E5430 at 2.67 GHz and 28 Gb RAM.

Fig. 18 shows the optimization results in the terms of ratios, in percentage, between the values of numerical and experimental natural frequencies (Fig. 18a), and MAC values (Fig. 18b), for the cases GA1 to GA4.

The figure shows that the errors associated with the frequencies are less than 5%, for the majority of the modes of vibration. Generally, the MAC values are higher than 0.90, and the values associated with the local modes are higher than the values of the global modes. The larger variability of the MAC values are associated with modes 4G, 6G and 11G.

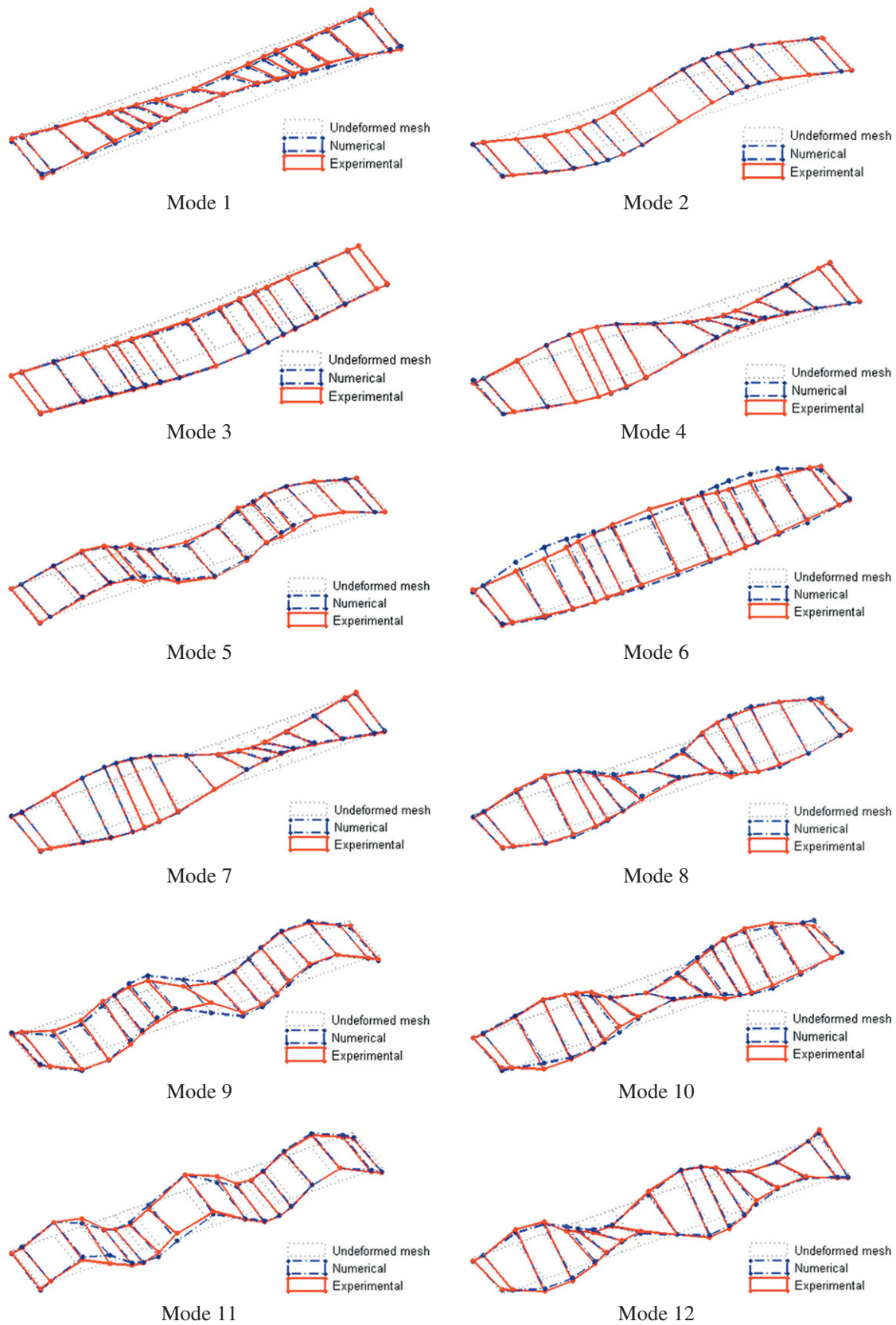
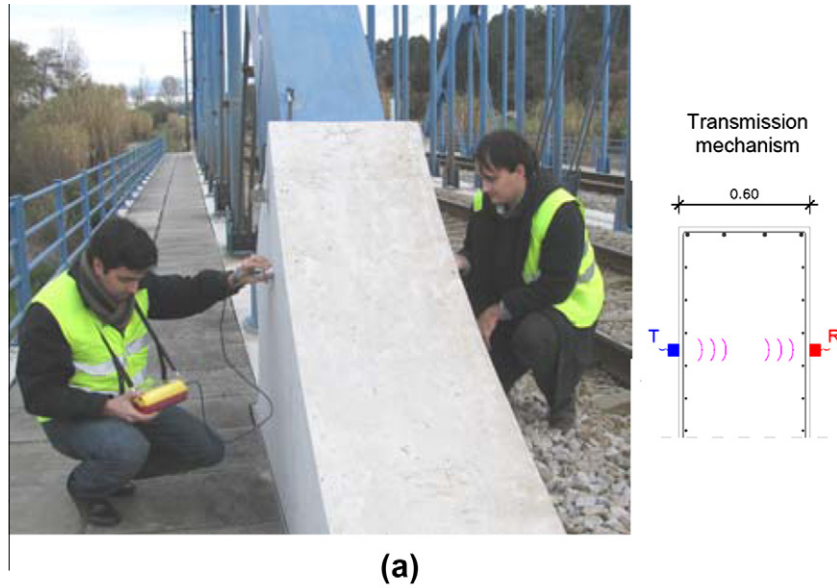


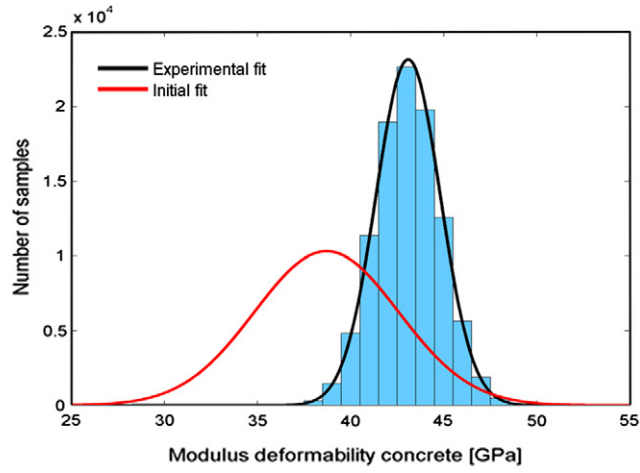
Fig. 22. Comparison between the experimental and numerical, after updating, mode shapes considering the optimization run GA2.

In general, the results for the different optimization runs are very similar, demonstrating the robustness of the genetic algorithm.

In Fig. 19 are represented the ratios of the values of each numerical parameter relative to the limits indicated in Table 1 for optimization runs GA1–GA4. A ratio of 0% means that the parameter

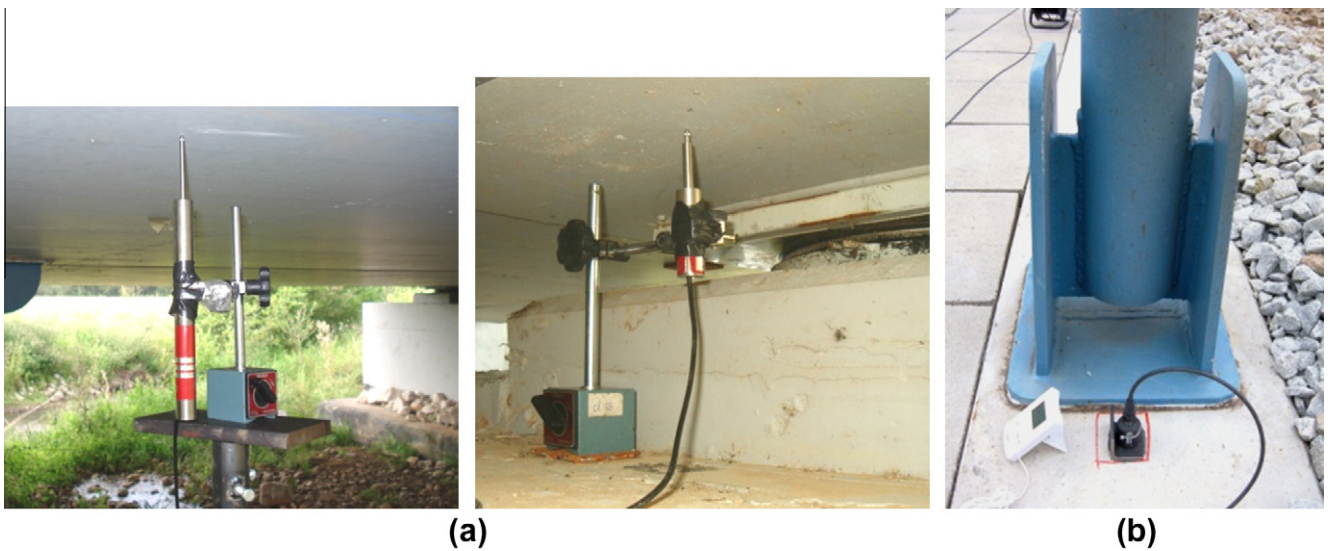


(a)



(b)

Fig. 23. Ultrasonic test: (a) layout and transmission mechanism, (b) estimate of the modulus of deformability of concrete.



(a)

(b)

Fig. 24. Dynamic test under railway traffic: (a) LVDT on the deck and nearby the support (b) accelerometer on the main girder of the deck.

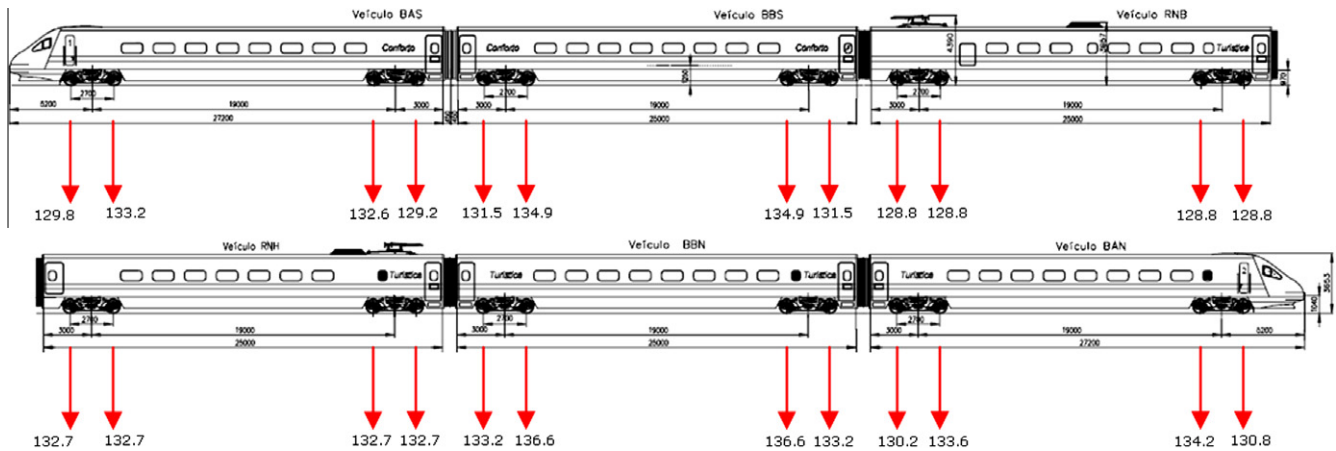


Fig. 25. Load scheme of alfa pendular train.

coincides with the lower limit. A ratio of 100% means that it coincides with the upper limit. The parameters that control the global modes are shown in Fig. 19a, with the values of the numerical parameters indicated in brackets.

The parameters that most influence the local modes are shown in Fig. 19b and c. The parameters that basically control the global modes, the modulus of deformability of concrete (E_c) and steel (E_s) and the vertical stiffness of the supports (K_v) presented lower variations, usually below 10%.

Concerning the densities of concrete and ballast, the different estimates showed higher variation, close to 20%. This is likely to be related to the fact that these parameters contribute similarly to the mass of the deck, and different combinations of these parameters may occur, leading to the same solution in terms of optimization of the problem.

Fig. 20 shows the error values between numerical and experimental frequencies, before and after calibration, taking as reference the values of the experimental frequencies. The results after calibration refer to the optimization run GA2, which is associated with the lowest residual of the objective function. The average error of the frequencies of global modes decreased from 4.7% before calibration, to 1.9% after calibration. In terms of the frequencies of local modes, the average error decreased from 7.5% before calibration, to 3.7% after calibration.

Fig. 21 shows a comparison of the MAC values of global modes (Fig. 21a) and local modes (Fig. 21b), before and after calibration of the numerical model.

For the case of the global modes, the average MAC value changed from 0.880, before calibration, to 0.908 after calibration. With regard to the local modes, the improvement was even more significant, as the average MAC value passed from 0.765, before the calibration, to a value of 0.974 after calibration. Fig. 22 presents a comparison of the experimental and numerical mode shapes after calibration.

6. Experimental validation

The validation of the numerical model of the bridge was carried out by ultrasonic tests, to characterize the modulus of deformability of concrete, and by a dynamic test under railway traffic.

6.1. Characterization of the modulus of deformability of concrete

The ultrasonic test [53] was performed based on a direct transmission technique [54]. Fig. 23a illustrates the execution of the test in the concrete block, with the schematic identification of the transmission mechanism.

The equipment consisted of an ultrasonic transmitter and receiver controlled by a central unit, model Proceq® Tico. The test was performed in seven different locations of the concrete block in a total of 19 individual measurements. The detection of the steel reinforcement rebars was performed using a laser system.

The distribution of the modulus of deformability of concrete (E_c) was estimated from the expression (adapted from [55]):

$$E_c = \frac{1}{k} \left[\frac{\rho_c(1 + \nu_c)(1 - 2\nu_c)}{(1 - \nu_c)} \left[\frac{l_1}{t} \right]^2 \right] \quad (4)$$

by means of a stochastic simulation, based on 10^5 samples, and considering the density of concrete (ρ_c) and the wave propagation time (t) as random variables. The estimated density of concrete assumed the values in the interval presented in Table 1. The dynamic Poisson's ratio of concrete was considered equal to 0.20. The width of the element had a value equal to 0.60 m. The measured wave propagation time varied between 127.3 and 127.6 μ s. The constant k performs the conversion of dynamic to static modulus of deformability of concrete and takes values between 1.12 and 1.25 [55].

The obtained results, presented in Fig. 23b, show that the modulus of deformability of concrete follows a normal distribution with mean value equal to 43.1 GPa and a coefficient of variation of 4.0%. Additional tests performed in the main girders of the deck conducted to estimates of the modulus of deformability of concrete similar to those obtained in the concrete block. In the same figure is included the distribution considered in the calibration of the numerical model (see Table 1) for concrete of the class C35/45 including the fly-ash addition. It can be pointed out that the values of the modulus of deformability of the concrete resulting from the optimization, with values between 44 and 45 GPa, fit the range of the most frequent values of the experimental distribution.

6.2. Dynamic test under railway traffic

The validation of the numerical model was also performed based on a dynamic test under railway traffic that consisted on the measurement of the dynamic response in terms of displacements and accelerations at several locations of the bridge deck.

Fig. 24 presents some details of the positioning of LVDTs for measuring the displacement in the reference section of the deck and in one of the supports (Fig. 24a), as well as an accelerometer also in the reference section of the deck (Fig. 24b).

The dynamic analyses were performed by the modal superposition method, using a moving loads methodology, considering the

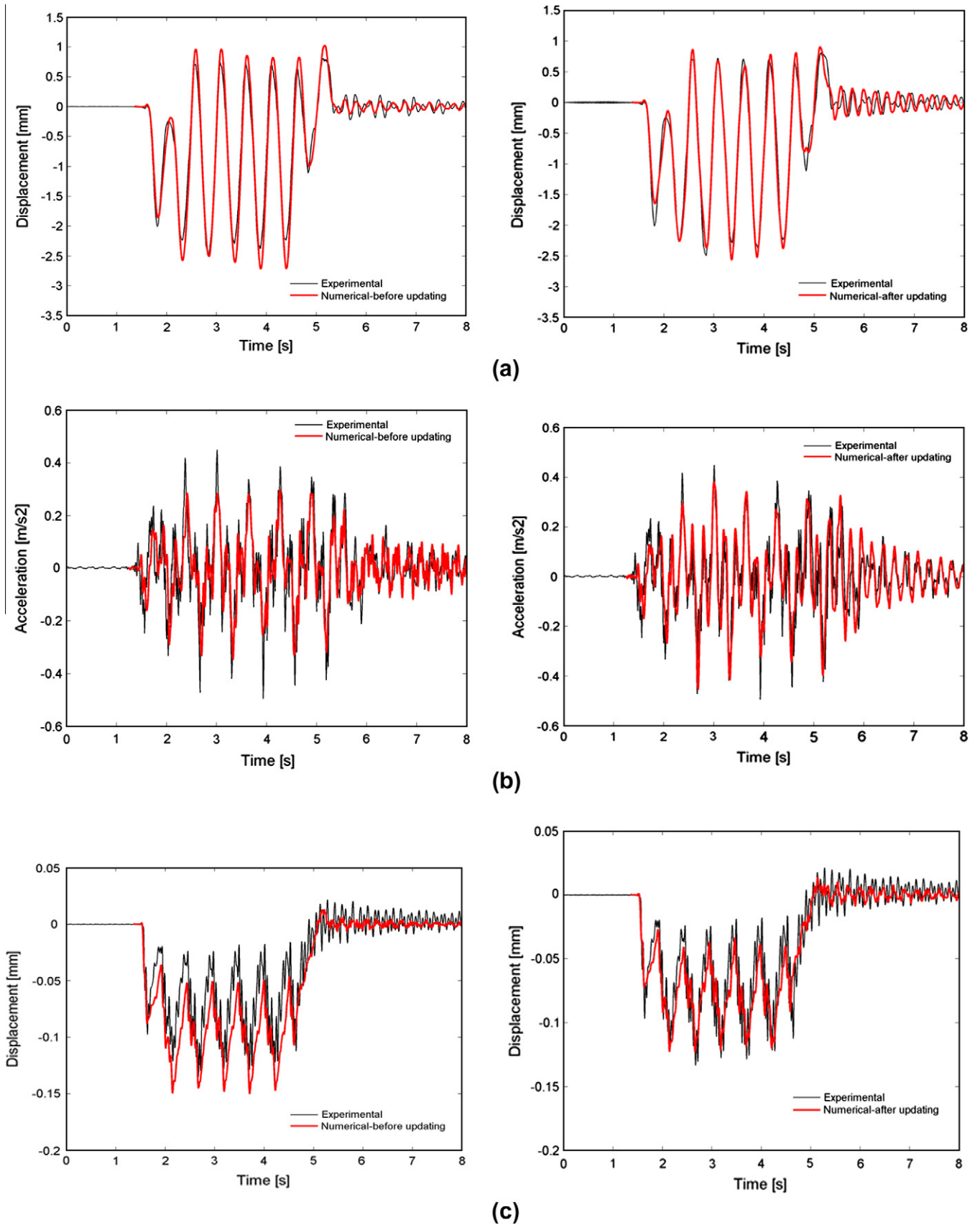


Fig. 26. Comparison of the experimental and numerical, before and after updating, dynamic responses of the bridge for the passage of alfa pendular train at a speed of 181 km/h: (a) displacements; (b) accelerations in the reference section of the deck; (c) displacements at the support.

modes of vibration with frequencies up to 30 Hz and an integration time increment equal to 0.001 s. The adopted modal damping coefficients were those experimentally obtained. The experimental acceleration records were filtered based on a low-pass digital filter with a cut-off frequency equal to 30 Hz.

Fig. 25 shows the load scheme of the alfa pendular tilting train. This conventional train has a total length of approximately 150 m and is composed by four motor vehicles (BAS, BBS, BBN and BAN) and two hauled vehicles (RNB and RNH). The axle loads varies between 128.8 and 138.4 kN.

Fig. 26 compares the dynamic responses of the bridge obtained by experimental and numerical calibration, before and after updating, for the passage of alfa pendular train at a speed (v) of 181 km/h. The dynamic response is compared in terms of displacement and acceleration in the position 11 of the bridge deck and also in terms of the displacement in the support.

The figures show a very good agreement between numerical, after updating, and experimental records. The dynamic responses, in particular in terms of displacement of the deck, are clearly dominated by the frequency associated with the passage of the regularly spaced groups of axles (f_g) with a spacing (d_g) of 25.9 m ($f_g = v/d_g = 181/3.6/25.9 = 1.96$ Hz). The response in terms of displacement of the support is also influenced by the frequency associated with the passage of successive axles (f_a) with constant distance (d_a) equal to 2.7 m ($f_a = v/d_a = 181/3.6/2.7 = 18.6$ Hz).

Regarding the response in terms of acceleration, it should be noted the important contribution of the frequency of the 2nd mode of vibration of the deck. In the experimental record, it is also possible to identify the contributions of frequencies above 20 Hz, possibly related with the irregularities of the track or wheels, causing the excitation of the axles or the bogies of the vehicles, which can only be simulated in a dynamic analysis including train-bridge interaction. The numerical results after updating revealed a better approximation to the experimental results, in comparison with the results before updating.

7. Conclusions

This paper described the calibration and experimental validation of a numerical model of a bowstring-arch railway bridge based on modal parameters. Based on an ambient vibration test and by the application of the EFDD method, the frequencies, mode shapes and damping coefficients of twelve global and local modes of vibration of the bridge were identified. A sensitivity analysis revealed that global modes are essentially influenced by the modulus of deformability and density of the concrete and by the modulus of deformability of the steel, the density of the ballast and the vertical stiffness of the supports. In contrast, the local modes are particularly sensitive to parameters related to the stress of the hangers and diagonals and to the stiffness of the elements that connect these elements to the arches and deck. The optimization of the numerical model was performed using a genetic algorithm and involved 15 numerical parameters and 48 modal responses (24 natural frequencies and 24 MAC values). The results of 4 optimization runs, based on different initial populations, led to very similar values of the frequencies, MAC and numerical parameters, which demonstrates the robustness of the genetic algorithm. The frequency differences with respect to the experimental values were generally below 5%. MAC values were found to be always above 0.85, and in the case of local modes, above 0.90. Concerning the numerical parameters, it is important to emphasize the stability of certain parameters, in particular the modulus of deformability of concrete and steel and the vertical stiffness of the supports, which presented variations of less than 10% within the considered range. Other parameters, such as the density of concrete and ballast, showed larger variability, close to 20%, which is related to the fact

that these parameters had a similar influence on the mass of the deck, and different combinations of these parameters may occur in order to obtain the same solution in terms of the optimization problem. The parameters related to the initial stress of the hangers and diagonals and the stiffness of the elements that make the connection to the arches and deck, with an important influence in the local modes, also showed variations below 20%. Comparing the values of the numerical frequencies of vibration before and after calibration, with the corresponding experimental values, significant improvements in the numerical model were found. The average error of the frequencies of vibration of global modes decreased from 4.7% before calibration to 1.9% after calibration. In the case of local modes there was also a significant improvement, considering the error evolution from 7.5% before calibration to 3.7% after calibration. In order to validate the optimization results, an ultrasound test was performed, which allowed measuring the modulus of deformability of the concrete, as well as a dynamic test under railway traffic, which allowed obtaining dynamic responses in terms of displacements, on the deck and support, and of acceleration of the deck. It was found that the values of the modulus of deformability of the concrete resulting from the optimization, between 44 and 45 GPa, fit in the range of most frequent values of the experimental distribution. A comparison of dynamic responses of the bridge for the passage of alfa pendular train at 181 km/h showed a very good agreement between numerical and experimental results. The small differences in the acceleration records are due to the contribution of frequencies above 20 Hz in the experimental record that were not present in the numerical record. This is possibly related with the irregularities of the track or wheels, causing excitation of the axis or bogies of the vehicles, and can only be simulated in a dynamic analysis with train-bridge interaction. The comparison between the experimental and numerical, before and after updating, dynamic responses revealed an important improvement of the correlation between records after updating.

The updated model will be used in the numerical simulation of the dynamic response for high-speed railway traffic in order to draw conclusions regarding the performance of the bridge in terms of structural safety (dynamic amplification and fatigue), track safety (track and wheel-track contact stability) and passengers comfort. Further research work in model updating is currently being developed namely in what concerns the inclusion of the dynamic responses in the objective function and also in the consideration of the uncertainties of the experimental data, such as frequencies and mode shapes, in the optimization problem.

Acknowledgements

The present work has been funded by the Portuguese Foundation for Science and Technology (FCT), in the context of the Research Project "Advanced methodologies for the assessment of the dynamic behaviour of high speed railway bridges" (FCOMP-01-0124-FEDER-007195). The first author, Ph.D. student, acknowledges the support provided by the European Social Fund, Programa Operacional da Ciência e Inovação 2010. The authors also would like to thank all the information provided by REFER, the company responsible for the management of the Portuguese railway network.

References

- [1] Frýba L, Pirner M. Load tests and modal analysis of bridges. *Eng Struct* 2001;23:102–9.
- [2] Marefat M-S, Gargary E, Ataei S. Load test of a plain concrete arch railway bridge of 20-m span. *Constr Build Mater* 2009;18:661–7.
- [3] Cunha Á, Caetano E, Calçada R, Roeck GD, Peeters B. Dynamic measurements on bridges: design, rehabilitation and monitoring. *Bridge Eng* 2003;156:135–48.

- [4] Jaishi B, Ren W-X. Structural finite element model updating using ambient vibration test results. *J Struct Eng* 2005;45:617–28.
- [5] Schlune H, Plos M, Gylltoft K. Dynamic finite element model updating of prestressed concrete continuous box-girder bridge. *Earthq Eng Eng Vib* 2009;31:1477–85.
- [6] Magalhães F, Cunha Á, Caetano E. Dynamic monitoring of a long span arch bridge. *Eng Struct* 2008;30:3034–44.
- [7] Benedettini F, Gentile C. Operational modal testing and FE model tuning of a cable-stayed bridge. *Eng Struct* 2011;33:2063–73.
- [8] Huang M, Guo W, Zhu H, Li L. Dynamic test and finite element model updating of bridge structures based on ambient vibration. *Front Archit Civil Eng China* 2008;2:139–44.
- [9] Wenzel H, Pichler D. Ambient vibration monitoring. West Sussex (UK): Wiley & Sons, Ltd.; 2005.
- [10] Zabel V, Brehm M. System identification of high-speed railway bridges. In: Gmbh D, editor. Weimar optimization and stochastic days 50 Weimar; 2009.
- [11] Chan THT, Li ZX, Yu Y, Sun ZH. Concurrent multi-scale modeling of civil infrastructures for analyses on structural deteriorating – Part II: Model updating and verification. *Finite Elem Anal Des* 2009;45:795–805.
- [12] Ewins DJ. Modal testing: theory and practice. London: Research Studies Press; 1984.
- [13] Friswell MI, Mottershead JE. Finite element model updating in structural dynamics. The Netherlands: Kluwer Academic Publishers; 1995.
- [14] Brehm M. Vibration-based model updating: reduction and quantification of uncertainties. Weimar (Germany): Bauhaus-Universität Weimar; 2011.
- [15] Yang YB, Chen YJ. A new direct method for updating structural models based on measured modal data. *Eng Struct* 2009;31:32–42.
- [16] Teughels A, Roeck GD, Suykens J. Global optimization by coupled local minimizers and its application to FE model updating. *Comput Struct* 2003;81:2337–51.
- [17] Cantieni R, Brehm M, Zabel V, Rauert T, Hoffmeister B. Ambient testing and model updating of a filler beam bridge for high-speed trains. In: 7th European conference on structural dynamics – EURO-DYN2008. Southampton, UK; 2008.
- [18] Zong Z-H, Jaishi B, Ge J-P, Ren W-X. Dynamic analysis of a half-through concrete-filled steel tubular arch bridge. *Eng Struct* 2005;27:3–15.
- [19] Chellini G, Salvatore W. Updated models for steel-concrete composite HS railway bridges. In: Conference experimental vibration analysis for civil engineering structures (EVACES). Porto, Portugal; 2007.
- [20] Liu W, Gao W, Sun Y, Xu M. Optimal sensor placement for spatial lattice structure based on genetic algorithms. *J Sound Vib* 2008;317:175–89.
- [21] Cantieni R, Brehm M, Zabel V, Rauert T, Hoffmeister B. Ambient modal analysis and model updating of a twin composite filler beam railway bridge for high-speed trains with continuous ballast. In: IMAC-XXVI conference on structural dynamics. Orlando, USA; 2008.
- [22] Teughels A. Inverse modelling of civil engineering structures based on operational modal data. Leuven (Belgium): Katolic University of Leuven; 2003.
- [23] Ren W-X, Chen H-B. Finite element model updating in structural dynamics by using the response surface method. *Eng Struct* 2010;32:2455–65.
- [24] Yu X, Gen M. Introduction to evolutionary algorithms. London (UK): Springer; 2010.
- [25] Brehm M, Zabel V, Bucher C. An automatic mode pairing strategy using an enhanced modal assurance criterion based on modal strain energies. *J Sound Vib* 2010;329:5375–92.
- [26] ANSYS. Structural analysis guide – release 11.0. In: ANSYS I, editor; 2007.
- [27] Henriques AAR. Aplicação de novos conceitos de segurança no dimensionamento do betão estrutural. Porto: Faculdade de Engenharia da Universidade do Porto; 1998.
- [28] Santos LO. Observação e análise do comportamento diferido de pontes de betão. Lisboa: Instituto Superior Técnico; 2001 [in Portuguese].
- [29] Wisniewski D. Safety formats for the assessment of concrete bridges. Guimarães: University of Minho; 2007.
- [30] UIC. Guidelines for railway bridges dynamic measurements and calculations. Bridcap project team G776x–2006. Paris: ETF – Railway Technical Publications; 2007.
- [31] JCSS. JCSS probabilistic model code Part 2: Load models. JCSS – Joint Committee on Structural Safety; 2001.
- [32] EN1992-1-1. Eurocode 2: Design of concrete structures. Part 1–1: General rules and rules for buildings. Brussels, Belgium: European Committee for Standardization; 2004.
- [33] UIC. UIC 719 R earthworks and track bed for railway lines; 2008.
- [34] EN1991-1-1. Eurocode 1: Actions on structures. Part 1–1: General actions – densities, self-weight, imposed loads for buildings. Brussels, Belgium: European Committee for Standardization; 2009.
- [35] Hess P, Bruchman D, Assakkaf I, Ayyub B. Uncertainties in material strength, geometric and load variables. *Naval Engineers Journal*; 2002.
- [36] UIC. UIC 864-5 O Specification technique pour la fourniture de semelles a poser sous rails; 1986.
- [37] Esveld C. Modern railway track. 2nd ed.; 2001.
- [38] REFER RFN. Projecto de Modernização da Linha do Norte – Substituição da ponte de São Lourenço ao km+158.662, Projecto de Execução, Memória Descritiva e Justificativa. Lisboa; 2003.
- [39] Toolbox TE. The engineering toolbox; 2011.
- [40] Lay MG. Handbook of road technology. 4th ed.; 2009.
- [41] Rinde JA. Poisson's ratio for rigid plastic foams. *J Appl Polym Sci* 1970;14:1913–26.
- [42] Johnson D. MatSE 406: thermal and mechanical behavior of materials In: Illinois M, editor; 2005.
- [43] Gent A, Suh J, Kelly III SG. Mechanics of rubber shear springs. *Int J Non-Linear Mech* 2007;42:241–9.
- [44] Fluorseals. Material specification – PTFE. In: Fluorseals, editor. Italy; 2006.
- [45] Rae PJ, Dattelbaum DM. The properties of poli(tetrafluoroethylene) (PTFE) in compression. *Polymer* 2004;45:7615–25.
- [46] Iman RL. Uncertainty and sensitivity analysis for computer modeling applications. In: Cruse TA, editor. Reliability Technology, The American Society of Mechanical Engineers; 1992. p. 153–68.
- [47] Iman RL, Conover WJ. A distribution-free approach to inducing rank correlation among input variables. *Commun Stat* 1982;B11:311–34.
- [48] ARTEMIS. ARTEMIS Extractor pro – academic licence. User's manual. In: ApS SVS, editor. Aalborg, Denmark; 2009.
- [49] Allemang RJ. The modal assurance criterion – twenty years of use and abuse. *J Sound Vib* 2003;37:14–21.
- [50] Saltelli A, Tarantola S, Campolongo F, Ratto M. Sensitivity analysis in practice. A guide to assessing scientific models. John Wiley & Sons, Ltd.; 2004.
- [51] Mathworks. MATLAB – getting started guide. Natick, USA; 2011.
- [52] OptiSLang. OptiSLang – the optimizing structural language. In: GmbH D, editor., 3.0 ed. Weimar, Germany; 2008.
- [53] Naik T, Malhotra M, Popovics J. The ultrasonic pulse velocity method. In: Press C, editor. Handbook on nondestructive testing of concrete; 2004.
- [54] EN12504-4. Testing concrete in structures. Part 4: Determination of ultrasonic pulse velocity. Brussels, Belgium: European Committee for Standardization; 2007.
- [55] BS – BS 1881–203. Testing concrete – Part 203: Recommendations for measurement of velocity of ultrasonic pulses in concrete. BSI; 1986.